Time-ordered-expression mRNA (TOE mRNA) for melanoma RNA vaccines

Supporting Information

Content

Supporting Methods

Materials

Primers for RT-qPCR, antibodies, chemical reagents, animals and cells used in this study are listed in **Table S1-S3**.

Plasmid construction

The pBFP-sensing-GFP (RE001) fluorescent protein plasmid encodes both blue fluorescent protein (BFP) and green fluorescent protein (GFP). The central sensing region targets exon 3 of EEF1A mRNA. The pBFP-sensingX-GFP (RE001X) plasmid was generated by substituting the TAG codon of pBFP-sensing-GFP (RE001) in the sensing region with TGG. The pAkaLuc-sensing-NanoLuc (TS002) luciferase plasmid encodes both AkaLuc and NanoLuc, derived by replacing BFP and GFP in the pBFP-sensing-GFP (RE001) plasmid with AkaLuc and NanoLuc, respectively. The pAkaLuc-SensingX (TS002X) plasmid was generated by substituting the TAG codon of the pAkaLuc-sensing-NanoLuc (TS002) in the sensing region with TGG. The plasmids for sequence optimization were constructed by replacing the human EEF1A mRNA exon 3 sensing region. Similarly, the pOVA-sensing-IL-12 (TS003) antigen-adjuvant plasmid encodes ovalbumin (OVA) and interleukin-12 (IL-12) proteins, with the central sensing region being mouse

EEF1A exon 3. Substitution of the TAG codon of the pOVA-sensing-IL-12 (TS003) in the sensing region with TGG yielded the pOVA-sensingX-IL-12 (TS003X) antigen-adjuvant plasmid. The pOVA (TS004) antigen plasmid expresses only the OVA antigen, while the pIL-12 (TS005) adjuvant plasmid expresses only the IL-12 adjuvant.

The pNeo-sensing-IL-12 (Neo001) antigen-adjuvant plasmid encodes the neoantigen (Pbk) and IL-12 adjuvants, with the central sensing region derived from mouse EEF1A exon 3. Replacing the TAG codon in the sensing region with TGG resulted in the pNeo-sensingX-IL-12 (Neo001X) antigen-adjuvant plasmid. The pNeo (Neo002) antigen plasmid expresses only the neoantigen protein, and the pIL-12 (Neo003) adjuvant plasmid expresses only the IL-12 adjuvant.

All plasmids were synthesized by General Biosystems (Anhui) Co., Ltd and uploaded to Genbank. Detailed construction information is listed in **Table S4-S6**.

Sensing sequence design and optimization

We employed the following strategy to design the sensing sequence: (1) Ensure complementarity to specific cellular coding or non-coding RNA sequences (trigger RNA); (2) Optimize the length to 200-300 nucleotides (nt); (3) Place different functional proteins upstream and downstream of the sensing sequence, ensuring they remain in the same continuous translational reading frame; (4) Include only one termination codon (TAG) at the center of the sensing sequence; (5) Identify a 5'-CCA-3' sequence in the trigger RNA that is complementary to the 5'-TGG-3' sequence in the sensing sequence, and replace the 5'-TGG-3' with 5'-TAG-3', maintaining an optimal length of 200-300 nt for the sensing sequence. Introduce an A-to-C mismatch when pairing with the trigger RNA; (6) Avoid the presence of ATG (start codon) after the TAG defined in step 5 to prevent unintended translation initiation; (7) Direct the sensing sequence to any region of the cellular transcript, including exons, introns, untranslated regions, or spliced mature mRNA; (8) Avoid sensing sequences with complex secondary structures.

The sensing sequences obtained through the above strategies can be further optimized by (1) targeting trigger RNAs with varying levels of gene expression within the cell and (2) selecting regions of the same trigger RNA that satisfy different design strategies. The optimization effect was evaluated by comparing

the expression time difference and relative expression levels in a luciferase system (TS002 mRNA) in HEK 293FT cells. Detailed information on the sensing sequences is provided in **Table S7**.

Cell culture and transfection

HEK293FT cells were maintained in complete DMEM medium (C11995500BT, Thermo) supplemented with 10% fetal bovine serum (FBS, 40130ES76, YEASEN), 1× non-essential amino acids (NEAA, 60707ES60, YEASEN), 1× GlutaMAX™ additive (35050061, Thermo), and 1× penicillin-streptomycin solution (60162ES76, YEASEN). Mouse B16F10 cells were cultured in complete RPMI 1640 medium (C11875500BT, Thermo) containing 10% FBS (40130ES76, YEASEN), 1× NEAA (60707ES60, YEASEN), 1× GlutaMAX™ additive (35050061, Thermo), and 1× penicillin-streptomycin solution (601050061, YEASEN). B3Z cells were cultured in B3Z medium composed of DMEM without sodium pyruvate (C11965092BT, Thermo), supplemented with 10% FBS (40130ES76, YEASEN) and 1× penicillin-streptomycin solution (60162ES76, YEASEN). All cell lines were cultured in a humidified incubator at 37°C with 5% CO_2. HEK293FT and B16F10 cells were obtained from the Cell Resource Center, Peking Union Medical College (PCRC), while B3Z cells were provided by Qingqi Biotechnology Development Co., Ltd. (Shanghai). All cell lines were authenticated by short tandem repeat (STR) profiling and tested negative for mycoplasma contamination.

When the cells reached 70%-80% confluence, plasmids were transfected into the cells using Hieff Trans® Liposomal Transfection Reagent (40802ES03, YEASEN), and mRNA was transfected using Hieff Trans® mRNA Transfection Reagent (40802ES03, YEASEN), following the manufacturer's instructions. Specifically, for plasmid transfection in 6-well plates seeded with HEK293FT cells: 30 min prior to transfection, the medium in each well was replaced with 2 mL of penicillin- and streptomycin-free culture medium. Subsequently, 1 μg of plasmid (RE001 or RE001X) was diluted in 250 μL of OPTI-MEM serum-reduced medium (31985070, Gibco) to prepare Solution A. In parallel, 2 μL of liposomal nucleic acid transfection reagent was diluted in 250 μL of OPTI-MEM serum-reduced medium to prepare Solution B. Solutions A and B were mixed in equal volumes, incubated at room temperature for 20 min, and then evenly added to the wells of the 6-well plates. For mRNA transfection in 6-well plates seeded with B16F10 cells: 30 min before transfection, the medium in each well was replaced with 2 mL of penicillin- and

streptomycin-free culture medium. Then, 1 μg of mRNA (TS002, TS002X, TS003, TS003X, TS004, TS005, or an equimolar mixture of TS004 and TS005) was diluted in 50 μL of OPTI-MEM serum-reduced medium (31985070, Gibco) to prepare Solution A. Solution B was prepared by diluting 2 μL of mRNA transfection reagent in 50 μL of OPTI-MEM serum-reduced medium. The two solutions were mixed in equal volumes, incubated at room temperature for 20 min, and then uniformly added to the wells of the 6-well plates. For experiments involving inhibitor treatment, an additional step was performed prior to transfection: 100 nM rapamycin (HY-10219, MCE), dissolved in DMSO (with the final DMSO concentration maintained ≤ 0.1% to avoid cytotoxicity), was added to the corresponding wells, followed by a 1-hour incubation.

Flow cytometry analysis

After a specified transfection period, the cells were harvested by trypsinization using trypsin (40127ES60, YEASEN), followed by centrifugation at 3000 rpm for 3 min. The supernatant was discarded, and the cells were resuspended in 250 μL of PBS (41403ES76, YEASEN). Subsequently, the cells were analyzed via flow cytometry (LSR Fortessa, BD Biosciences). Data acquisition was performed using FACSDIVA software (BD Biosciences), and data analysis was conducted using FlowJo v10 (FlowJo). For cell surface OVA detection, primary antibody against ovalbumin (sc-65984, Santa Cruz Biotechnology, diluted 1:200) was incubated with the cells for 1 h according to the manufacturer's instructions. This was followed by the addition of the secondary antibody Alexa Fluor 647 AffiniPure Goat Anti-Mouse IgG (H+L) (33213ES60, YEASEN, diluted 1:500) for 0.5 h. The cells were then collected and processed similarly for further analysis. For multiparametric flow cytometry analysis of DC maturation, immune model, and tumor model, detailed antibody information is provided in **Table S1**. Similar procedures were applied for sample cell processing using a full-spectrum flow cytometric analyzer (LE-ID7000C, SONY). Data collection was performed using ID7000 Software Analysis Mode (SONY), and data analysis was conducted using FlowJo v10 (FlowJo).

Fluorescence imaging

HEK293FT cells were transfected with 1 μg of RE001 or RE001X plasmid in 6-well plates. Cellular expression of fluorescent proteins was monitored at 0, 8, 12, 24, 36, 48, 60, 72, 84, and 96 hours post-transfection using the BFP and GFP channels of the EVOS FL Imaging System (EVOS FL Auto, Thermo).

A-to-I editing rate by time-course detection

To evaluate the time-course A-to-I editing rate, HEK 293FT cells were seeded in 12-well plates. At the indicated time post-transfection, cells were collected separately and total RNA was extracted using the RNA Easy Fast Tissue/Cell Kit (DP451, TIANGEN). Extracted RNAs were converted to cDNA using Hifair® II 1st Strand cDNA Synthesis SuperMix (1119ES60, YEASEN). PCR products covering the target sensing sequence region were generated with 2× Hieff Canace® PCR Master Mix (10136ES, YEASEN), and purified with a Tiangen Gel Purification Kit (4992984, TIANGEN) for Sanger sequencing. At each time point, editing efficacy was calculated as the ratio of Sanger peak heights G/(A + G). Three biological replicates were performed for each time point.

Luciferase reporter assay

HEK293FT cells were transfected with 1 μg of either TS002 or TS002X mRNA in a 6-well plate. After 24 hours, the cells were washed twice with pre-chilled 1× PBS (4°C, 41403ES76, YEASEN). Subsequently, 100 μL of lysis buffer (20118ES60, YEASEN, supplemented with 1 mM PMSF (BN20393, BIORIGIN)) was added to each well to lyse the cells. The lysates were further disrupted using ultrasonication at 80% intensity with a duty cycle of 3 seconds on and 9 seconds off for a total duration of 16 minutes (Q800R3 sonicator, Qsonica). The samples were then centrifuged at 14,000 rpm for 15 minutes at 4°C, and the supernatant was collected as the total protein extract.

Two luciferase assay systems were prepared as follows: For the luciferase assay system, 80 μL of 10 mM Mg-ATP (R21326, Shanghai Yuanye Bio-Technology), 8 μL of 5 mM akalumine substrate (HY-112641A, MCE), and 0.2 M Na_3PO_4 (BN24319, BIORIGIN) were mixed, and the final volume was adjusted to 1 mL with H_2O. For the Nanoluciferase Assay System, 2 μL of 0.5 M EDTA (AM9260G, Thermo), 150 μL of 1 M KCl (FB9997-500, FeiMoBio), 100 μL of 100 mM DTT (1758-9030, INALCO), 5 μL of NP-40 (20103ES60, YEASEN), and 1 μL of 20 mM furimazine substrate (M10519, AbMole) were combined, and the final volume was adjusted to 1 mL with H_2O. Equal volumes (10 μL) of each luciferase assay system

solution and the protein extract were added to the wells of a 384-well full white polystyrene microplate (142762, Thermo). The mixture was thoroughly mixed using a SPARK multimode microplate reader (Spark, TECAN), and luminescence signals from Akaluciferase (640-665 nm) and Nanoluciferase (430-470 nm) were immediately detected.

In vitro transcription

For in vitro or in vivo experiments, the corresponding plasmids were linearized by enzymatic digestion using the restriction endonuclease AflII (R0520V, NEB). The linearization reaction mixture consisted of 20 μg of plasmid, 10 μL of AflII enzyme, and 10 μL of 10× rCutSmart Buffer (B6004S, NEB) in a total volume of 100 μL. The reaction was incubated at 37°C for 1 hour. The linearized DNA was subsequently purified from the gel using a Tiangen Gel Purification Kit (4992984, TIANGEN). A total of 5 μg of purified linearized DNA was diluted to 40 μL and used as a template for an in vitro transcription system. The transcription reaction mixture contained 10 μL of 10× Transcription Buffer (10618ES90, YEASEN), 5 μL of T7 RNA polymerase (10618ES90, YEASEN), 0.2 μL of pyrophosphatase (10658ES10, YEASEN), 2.5 μL of RNase inhibitor (R301-01, Vazyme), 2.3 μL of 1× storage buffer, 40 μL of 100 mM ribonucleoside triphosphates (rNTPs) (N0466S, NEB), and 5% N1-methyl-pseudouridine (ψ) (10651ES20, YEASEN). This mixture was incubated at 37°C for 2 hours. Following transcription, DNase I (10325ES80, YEASEN) was added to digest the template DNA at 37°C for 30 minutes. The mRNA was then purified via ethanol precipitation.

A solution containing 50 μg of mRNA was diluted to 46.25 μL and subjected to a thermal cycle at 65°C for 5 minutes, followed by cooling on ice for 5 minutes. A capping reaction mixture (53.75 μL) was prepared, consisting of 5 μL of 10 mM GTP (10132ES03, YEASEN), 6.25 μL of 8 mM S-adenosylmethionine (SAM) (10619ES02, YEASEN), 2.5 μL of RNase inhibitor (R301-01, Vazyme), 25 μL of Vaccinia capping enzyme (10614ES84, YEASEN), 10 μL of 10× capping buffer (10666ES03, YEASEN), and 5 μL of 2'-O-methyltransferase (10612ES92, YEASEN). The 46.25 μL of mRNA was added to this capping mixture and incubated at 37°C for 2 hours. After capping, the mRNA was purified again via ethanol precipitation, and the concentration of the purified RNA was determined using a NanoDrop 2000 spectrophotometer (Thermo).

ELISA

Cell culture supernatants were collected, and the concentrations of target molecules in the supernatants were quantified using commercially available kits according to the manufacturers' instructions. Specifically, mouse IL-12p70 levels were measured using an IL-12p70 ELISA Kit (BN50536, BIORIGIN), and mouse IFN-γ levels were determined using an IFN-γ ELISA Kit (BN50528, BIORIGIN).

Serum samples from mice were collected and appropriately diluted as per the manufacturer's guidelines. Subsequently, the levels of target molecules in the serum were assessed using specific assay kits. In detail, mouse IFN-β levels were quantified using the IFN-β ELISA Kit (EM1148, FineTest), mouse IFN-γ levels were measured using the IFN-γ ELISA Kit (EM0093, FineTest), mouse IL-2 levels were determined using the IL-2 ELISA Kit (EM0112, FineTest), mouse IL-4 levels were quantified using the IL-4 ELISA Kit (EM0119, FineTest), OVA-specific IgA levels were evaluated using the OVA sIgA ELISA Kit (EM2036, FineTest), OVA-specific IgG, IgG1, and IgG2a levels were measured using their respective ELISA Kits (EM1255, EM1996, and EM1997, FineTest), and OVA concentrations were determined using the Ovalbumin ELISA Kit (abx259051, Abbexa).

Cell line construction

Stable ADAR1 gene-knockdown and ADAR1-overexpressing cell lines were established through le ntiviral transfection followed by drug selection. For the knockdown cell line, the shRNA lentiviral expression plasmid was obtained from the Core Facility, Center of Biomedical Analysis, Tsinghua University, with the following TRC ID: TRCN0000050791 and OLIG_SEQ: ACTTTGAACTCGA GTTCAAAGTCAACATAC-CCTGCTTTTTG. For the overexpression cell line, the lentiviral expre ssion plasmid (pLV-ADAR1p150-Puro) was synthesized by General Biosystems (Anhui) Co., Ltd..

The procedure for lentivirus production involved the following steps: HEK293FT cells were cultured to 80%-90% confluence in a 6-well plate. Two hours prior to transfection, the medium in each well was replaced with 2 mL of OPTI-MEM reduced serum medium (31985070, Gibco). The target plasmid (0.5 μg), pMD2.G plasmid (0.5 μg), and pSAX2 plasmid (0.5 μg) were separately diluted in 250 μL of OPTI-MEM reduced serum medium to form Solution A. Meanwhile, 3 μL of lipid transfection reagent was diluted in another 250 μL of OPTI-MEM medium to form Solution B. Solutions A and B were mixed in equal

volumes and incubated at room temperature for 20 minutes before being gently added to the cells. At 24 hours and 72 hours post-transfection, the culture supernatants were collected, centrifuged at 2000 rpm for 10 minutes, and filtered through a 0.45 μm filter to generate lentiviral stocks, which were stored at -80°C.

To establish the ADAR1-knockdown and ADAR1-overexpressing cell lines, HEK293FT cells were grown to 70%–80% confluence, and the medium was replaced with lentiviral transduction medium. This medium consisted of 200 μL of lentiviral stock, 1800 μL of standard growth medium, and 1.6 μL of polybrene (40804ES76, YEASEN). After 48 hours of stable transduction, the medium was replaced with medium containing 2 μg/mL puromycin for selection. The selection process continued for seven days, after which the surviving cells represented the target cell lines. The knockdown or overexpression efficiency was validated using real-time fluorescence quantitative PCR (qPCR) and Western blot analysis.

Generation of murine bone marrow-derived dendritic cells

8- to 10-week-old C57BL/6 mouse femurs and tibias were isolated and placed in Petri dishes containing 75% ethanol. The bones were subsequently rinsed twice with PBS and transferred to fresh PBS-filled dishes. The ends of the bones were trimmed using a surgical blade, and the bone marrow contents were flushed into a centrifuge tube containing 3 mL of PBS using a 2-mL syringe filled with PBS. This process was repeated 4-5 times at each end to obtain a cell suspension. The cell suspension was centrifuged at 300 × g for 5 minutes, the supernatant was discarded, and the cells were resuspended in 1 mL of red blood cell lysis buffer (40401ES60, YEASEN) for 5 minutes. After lysis, 9 mL of PBS was added to neutralize the lysis buffer, followed by another centrifugation step at 300 × g for 5 minutes. The supernatant was removed, and the cells were resuspended in 10 mL of culture medium composed of RPMI-1640 (C11875500BT, Thermo), L-glutamine, 10% FBS (40130ES76, YEASEN), 1% nonessential amino acids (60162ES76, YEASEN), 10 mM HEPES (60117ES60, YEASEN), 50 μM β-mercaptoethanol (M131, Amresco), and 5% penicillin/streptomycin (60162ES76, YEASEN). The cell suspension was filtered through a 40-μm filter (CSS013040, BIOFIL), and cell viability was assessed by mixing 20 μL of the suspension with 20 μL of Trypan blue (ST798, Beyotime) for 3-7 minutes. Viable cell counts were determined using a Nexcelom Cellometer automated cell counter.

The cells were adjusted to a density of 1×10^6 cells/mL in culture medium supplemented with 15 ng/mL GM-CSF (91108ES08, YEASEN) and 10 ng/mL IL-4 (P07750, Novoprotein). The cells were plated in 6-well plates at a volume of 3 mL per well under conditions of 37°C, 5% CO_2, and 95% humidity in a CO_2 incubator, marking the first day of cultivation. On day 3, the medium was removed, the wells were rinsed with 2 mL of fresh PBS, and nonadherent cells were gently removed by tilting the plate. On day 5, fresh medium containing 15 ng/mL GM-CSF and 10 ng/mL IL-4 was added to the wells to continue the culture process. On day 7, an additional 3 mL of fresh medium supplemented with cytokines was added to each well. The entire 6-well plate was then placed on ice for 10 minutes, after which the medium was carefully aspirated to harvest the loosely adherent BMDCs.

RT-qPCR

BMDCs were seeded in a 6-well plate, and 24 hours after transfection with the respective mRNAs, the cells reached 70%-80% confluency. Total RNA was extracted from these cells using the RNA Easy Fast Tissue/Cell Kit (DP451, TIANGEN). First-strand cDNA synthesis was performed using Hifair® II 1st Strand cDNA Synthesis SuperMix (11119ES60, YEASEN) on a PCR instrument (ProFlex PCR System, Thermo). Quantitative real-time PCR (qPCR) was subsequently conducted according to the manufacturer's instructions, using Hieff® qPCR SYBR Green Master Mix (11201ES03, YEASEN) on a qPCR machine (CFX96, BIO-RAD). The primers used for qPCR are listed in **Table S3**. Each gene was analyzed in quadruplicate, and real-time fluorescence data were collected to calculate threshold cycle (Ct) values automatically by the instrument. Mean Ct values were derived from triplicate measurements for further analysis. Relative expression levels of the target genes were calculated using the $2^{-\Delta\Delta Ct}$ method, with Gapdh serving as the reference gene. Data analysis was performed using Microsoft Excel (Microsoft Corp.) and GraphPad Prism 9 (GraphPad Software). For the detection of trigger RNA perturbation, similar detection steps were followed, with GAPDH used as the reference gene.

To validate the regulation of ADAR1 in cells, ADAR1-overexpressing, wild-type (WT), and ADAR1-knockdown cells were seeded in a 6-well plate. In this case, β-actin (ACTB) served as the internal control, and all other procedures were identical to those described above.

Western blotting

The cells were cultured in a 6-well plate and washed twice with prechilled PBS (4°C, 41403ES76, YEASEN). Subsequently, 100 μL of lysis buffer for Western blotting and immunoprecipitation (WB/IP) (20118ES60, YEASEN, supplemented with 1 mM PMSF (BN20393, BIORIGIN)) was added to each well to lyse the cells. The cell lysate was further disrupted by ultrasonication at 80% intensity with cycles of 3 seconds on and 9 seconds off for a total of 16 minutes using a Q800R3 sonicator (Qsonica). After centrifugation at 14,000 rpm for 15 minutes at 4°C, the supernatant was collected as the total protein extract. Protein concentrations were quantified using a BCA protein assay kit (20200ES76, YEASEN), ensuring that equal amounts of protein (20 μg) were loaded per lane for electrophoresis. Proteins were resolved via a 15% high-resolution precast gel (36248ES10, YEASEN) and transferred onto a nitrocellulose (NC) membrane. The NC membrane was washed three times with 1× TBST (TBS buffer containing 0.05% Tween 20), blocked for one hour at room temperature in TBST containing 5% skim milk, and washed three more times with TBST. The primary antibody mixture was incubated at room temperature for one hour, followed by three washes with TBST. The secondary antibody mixture was subsequently incubated at room temperature for another hour, after which the samples were washed three times with TBST. Equal volumes of solutions A and B from the ECL Chemiluminescent Substrate Kit (36222ES76, YEASEN) were mixed and evenly applied to the membrane. The chemiluminescent signal was promptly detected using a smart imaging workstation (GelView 6000Plus, BLT), and the data were analyzed using ImageJ (National Institutes of Health).

To detect ADAR1 protein expression, the primary antibody anti-ADAR1 (sc-73408, Santa Cruz Biotechnology, diluted 1:200) and the secondary antibody goat anti-mouse IgG H&L/HRP (bs-60296G-HRP, Bioss, diluted 1:2000) were used. For the internal reference protein β-actin, a rabbit anti-β-actin polyclonal antibody (30102ES60, YEASEN, diluted 1:2000) and a goat anti-rabbit IgG H&L (HRP) antibody (ab6721, Abcam, diluted 1:2000) were employed.

To detect the self-cleaving activity of the 2A peptide, the following antibodies were used: an EBFP Mouse mAb (bsm-33185M, Bioss, diluted 1:1000) and a goat anti-mouse IgG H&L/HRP (bs-60296G-HRP, Bioss, diluted 1:2000) for BFP detection; a GFP antibody (HY-P80141, MCE, diluted 1:200) and a goat anti-rabbit IgG H&L (HRP) antibody (ab6721, Abcam, diluted 1:2000) for GFP detection; an anti-firefly luciferase antibody (ab181640, Abcam, diluted 1:1000) and a Donkey anti-Goat IgG H&L antibody (ab216775,

Abcam, diluted 1:1000) for AkaLuc detection; an Anti-NanoLuc® Monoclonal Antibody (N700A, Promega, diluted 1:500) and a goat anti-mouse IgG H&L/HRP (bs-60296G-HRP, Bioss, diluted 1:2000) for NanoLuc detection; an OVA antibody (sc-65984, Santa Cruz Biotechnology, diluted 1:200) and a goat anti-mouse IgG H&L/HRP (bs-60296G-HRP, Bioss, diluted 1:2000) for OVA detection; and an IL-12B p40 antibody (sc-57258, Santa Cruz Biotechnology, diluted 1:200) and a Peroxidase AffiniPure Goat Anti-Rat IgG (H+L) (33301ES60, YEASEN, diluted 1:2000) for IL-12 detection.

To detect the activated key proteins in the mTORC1 pathway, the following antibodies were used: a 4E-BP1 antibody (sc-9977,Santa Cruz Biotechnology, diluted 1:200) and a goat anti-mouse IgG H&L/HRP (bs-60296G-HRP, Bioss, diluted 1:2000) for the total 4E-BP1 detection; a p-4E-BP1 antibody (sc-293124,Santa Cruz Biotechnology, diluted 1:200) and a goat anti-mouse IgG H&L/HRP (bs-60296G-HRP, Bioss, diluted 1:2000) for the phosphorylated 4E-BP1 detection; an S6K1 antibody (sc-8418,Santa Cruz Biotechnology, diluted 1:200) and a goat anti-mouse IgG H&L/HRP (bs-60296G-HRP, Bioss, diluted 1:2000) for the total S6K1 detection; a p- S6K1 antibody (sc-8416,Santa Cruz Biotechnology, diluted 1:200) and a goat anti-mouse IgG H&L/HRP (bs-60296G-HRP, Bioss, diluted 1:2000) for the phosphorylated S6K1 detection; For the internal reference protein β-actin, a rabbit anti-β-actin polyclonal antibody (30102ES60, YEASEN, diluted 1:2000) and a goat anti-rabbit IgG H&L (HRP) antibody (ab6721, Abcam, diluted 1:2000) were employed.

RNA-seq

BMDCs were seeded into 6-well plates and transfected with the corresponding mRNAs, with three technical replicates prepared for each group. At 24 hours post-transfection, when the cell confluence reached 70%-80%, the cells were washed twice with pre-chilled 1× PBS (4°C). Subsequently, 1 mL of Biozol Total RNA Extraction Reagent (BN20537, BIORIGIN) was added to each well to extract total RNA. RNA sequencing (RNA-Seq) experiments on the collected samples were performed by Shanghai Liebing Information Technology Co., Ltd. Following sequencing, the raw data were processed and analyzed by Shanghai Liebing Information Technology Co., Ltd., providing comprehensive insights into the transcriptomic profiles induced by the mRNA transfections. All data were uploaded to GEO with accession number: GSE279604.

Ribosome RIP–qPCR

BMDCs were seeded into 6-well plates and transfected with the respective mRNAs, with three technical replicates prepared for each condition. At 24 hours post-transfection, when the cell confluence reached 70%-80%, the cells were harvested by trypsin digestion and resuspended in PBS. For each sample, ribosome-bound mRNA was extracted using the EzraBio Kit (QEZ-seq® Version 1.0, NeoRibo). Parallel samples were processed for total RNA extraction using Biozol Total RNA Extraction Reagent (BN20537, BIORIGIN). Both ribosome-nascent-chain-complex (RNC) mRNA and total RNA were subsequently subjected to RT-qPCR analysis, with Actb serving as the housekeeping gene for calculating the relative level of the target gene OVA. The data were analyzed using Microsoft Excel and GraphPad Prism 9. The translation efficiency (TE) was calculated via the following formula:

$$\mathrm{TE}(\%) = \frac{\text{Relative RNC mRNA expression}}{\text{Relative total mRNA expression}} \times 100$$

Cytometric bead array (CBA)

The quantitative detection of various cytokines produced after mRNA transfection into BMDCs was conducted as follows: BMDCs were seeded in 6-well plates and transfected with 1 μg of mRNA, specifically TS003, TS003X, TS004, TS005, or an equimolar mixture of TS004 and TS005, using the previously described transfection methodology. On the following day, the culture supernatants from each well were harvested by centrifuging the samples at 300 × g for 5 minutes to remove any remaining cells.

The concentrations of IL-10, MCP-1, IFN-γ, TNF, and IL-12p70 in the collected supernatants were quantified using a BD™ Cytometric Bead Array (CBA) Mouse Inflammation Kit (552364, BD) according to the manufacturer's instructions. Data acquisition during the cytokine detection process was performed using FACSDIVA Software (BD Biosciences). The resulting data were then analyzed in detail using FlowJo v10 software (FlowJo LLC).

B3Z hybridoma assay

A 96-well plate was seeded with BMDCs at a density of 1×10^5 cells/100 μL. The cells were then transfected with 1 μg of in vitro transcribed mRNA from each group, including TS003, TS003X, TS004,

TS005, or an equimolar mixture of TS004 and TS005. Each group consisted of three technical replicates. Twenty-four hours post-transfection, B3Z cells were added to each well at a density of 1×10^5 cells/100 μL, and co-cultivation was continued for an additional 24 hours. Following the co-culture period, the medium was aspirated, and the wells were washed twice with PBS.

Subsequently, 100 μL of CPRG (chlorophenol red-β-D-galactopyranoside) coloration solution was added to each well. This solution consisted of 0.12 mM CPRG (GC47080, GlpBio) and 100 mM β-mercaptoethanol (M131, Amresco) dissolved in PBS and was incubated at 37°C for 4 hours, during which a noticeable color change occurred. Next, 100 μL of lysis buffer containing 9 mM $MgCl_2$ (NR0220, Leagene) and 0.125% NP-40 (20103ES60, YEASEN) dissolved in PBS was added to each well, followed by incubation at 37°C for 4 hours. Subsequently, 100 μL of CPRG stop solution (containing 300 mM glycine (G8200, Solarbio) and 15 mM EDTA (AM9260G, Thermo)) was added to each well, and the contents were gently mixed to ensure homogeneity. Finally, the absorbance at 570 nm was quantified using a multilabel microplate reader (PerkinElmer) to determine β-galactosidase activity, reflecting the activation of B3Z cells due to antigen presentation by BMDCs. This assay serves as an indicator of the antigen presentation efficiency of the transfected BMDCs to the T-cell hybridoma B3Z.

In vitro T-cell proliferation assay

BMDCs were seeded in 6-well plates and transfected with 1 μg of in vitro transcribed mRNA for each type: TS003, TS003X, TS004, TS005, or an equimolar mixture of TS004 and TS005, following the established protocol. The following day, 8- to 12-week-old OT-I mice were euthanized via CO_2 asphyxiation. The spleens were harvested, thoroughly homogenized, and passed through a 40-μm cell strainer (CSS013040, BIOFIL) to isolate single-cell suspensions, which were then washed with prechilled PBS (4°C). Centrifugation at 300 × g for 5 minutes at 4°C was performed to remove the supernatant. Subsequently, 1 mL of red blood cell lysis buffer (40401ES72, YEASEN) was added, and the suspension was incubated at room temperature for 3 minutes before being centrifuged again under the same conditions to discard the supernatant. The cell pellets were resuspended in MACS Running Buffer, which consisted of PBS supplemented with 0.5% bovine serum albumin (BSA) and 2 mM EDTA.

In accordance with the manufacturer's instructions, $CD8^+$ T cells were negatively isolated using antibody-conjugated magnetic beads (8804-6822, Thermo) and subsequently resuspended in complete RPMI 1640 medium. The $CD8^+$ T cells were stained according to the guidelines provided in the CellTrace™ CFSE Cell Proliferation Kit (C34570, Thermo) to label them with CFSE for tracking proliferation. Following the staining procedure, 2×10^6 cells were resuspended in 500 μL of media and co-cultured with BMDCs in 6-well plates. After 24 hours of co-culture, T-cell proliferation was assessed via flow cytometry.

The T-cell proliferation ratio was determined via the following formula:

$$\text{T cell proliferation}(\%) = \frac{\text{count CFSE}^{\text{low}}}{\text{count CFSE}^{\text{high}} + \text{count CFSE}^{\text{low}}} \times 100$$

Animals and vaccine injection

For the experiments, 6- to 8-week-old C57BL/6 mice were procured from Beijing Vital River Laboratory Animal Technology Co., Ltd. and housed in Phase I of Tsinghua University's Experimental Animal Center under specific pathogen-free (SPF) conditions. All animal experimental protocols were approved by Tsinghua University's Institutional Animal Care and Use Committee (IACUC) with the Animal Protocol number 23-LJH4. OT-I mice were obtained from Shulaibao (Wuhan) Biotechnology Co., Ltd.

The mRNA vaccine preparation utilized in this study involved in vitro transcription (as previously described) and encapsulation of the mRNA. The concentration of the transcribed mRNA was measured using a NanoDrop 2000 spectrophotometer (Thermo) and adjusted to a final concentration of 1 μg/μL. Mice were intravenously injected with the mRNA vaccine in a volume of 100 μL containing 10 μg of mRNA. The mRNA was encapsulated and delivered via SM-102 (HY-134541, MCE) LNPs, which were freshly prepared immediately before use according to the manufacturer's instructions using the NanoAssemblr Benchtop instrument (Precision). Briefly, mRNA was diluted to 0.1–0.35 mg ml^{-1} in RNase-free water containing 25 mM sodium acetate (pH 5.0) as the aqueous phase. The lipid phase, formulated to achieve an N:P ratio of 6:1, consisted of SM-102, DSPC (Avanti, 850365), cholesterol (Sigma, C8667), and PEG2000 PE (Avanti, 880150) dissolved in ethanol at a molar ratio of 50:10:38.5:1.5. The aqueous and lipid phases were loaded into separate syringes at a 3:1 volume ratio, transferred to a pre-washed NanoAssemblr Benchtop Acetone Cartridge (Precision, NIT0058), and mixed at a flow ratio of 3:1 and

flow speed of 6 ml min^{-1} to generate LNPs. Post-formulation, LNPs underwent buffer exchange to PBS via dialysis and concentration by ultrafiltration, followed by characterization: mRNA encapsulation efficiency and concentration were determined using the Quant-iT RiboGreen RNA Assay kit (Thermo Fisher, R11490). Particle size and polydispersity (PDI) were analyzed via dynamic light scattering (Zetasizer Pro, Malvern Panalytical) in PBS, while zeta potential was measured with the same instrument in double-distilled water. The size data is reported as the largest intensity mean peak average, accounting for >95% of the nanoparticles in the sample. Finally, LNPs were sterilized by filtration and used immediately. The control group of mice received an equivalent volume of saline.

In vivo immunity assay in mice

In the experiment, 6- to 8-week-old C57BL/6 mice were intravenously injected via the tail vein with 100 μL containing 10 μg of in vitro transcribed mRNA vaccines—TS003, TS003X, TS004, and TS005—or an equimolar mixture of TS004 and TS005—or 100 μL of physiological saline as a control, marking day 0. A second immunization with the same dosage was administered on day 21, with five parallel control mice established for each group.

Blood serum was collected from the mice on days 0, 1, 3, 7, 14, 21, 22, and 42. ELISA kits were used to quantify the levels of anti-OVA IgA, anti-OVA IgG, anti-OVA IgG1, and anti-OVA IgG2a antibodies, as well as the levels of the cytokines IL-2, IL-4, IFN-γ, and IFN-β in the serum.What's more, the whole blood samples were analyzed for blood biochemistry and hematology to assess overall physiological status.

Additionally, spleens, lungs, and lymph nodes were harvested from the mice on the specified days. The organs were minced thoroughly, filtered through a 40-μm cell strainer (CSS013040, BIOFIL) to obtain single-cell suspensions, and washed with prechilled PBS (4°C). After centrifugation at 300 × g for 5 minutes at 4°C to remove the supernatant, 1 mL of red blood cell lysis buffer (40401ES72, YEASEN) was added, and the suspension was incubated at room temperature for 3 minutes. This was followed by another round of centrifugation and removal of the supernatant. Cells from each mouse's three organs were subsequently distributed at a 1:3 ratio for the assessment of T-cell and innate immune cell responses.

The cells derived from organ dissociation were resuspended in 100 μL of a cocktail of antibodies, with the amounts adjusted according to the manufacturer's instructions (details of the antibodies are listed in

Supporting Table S1). Following an incubation period of one hour in the dark on ice, the cells were centrifuged, washed twice with PBS, fixed with 100 μL of 4% paraformaldehyde (PFA), centrifuged again, and finally resuspended in 200 μL of PBS. Full-spectrum flow cytometry analysis was conducted using an LE-ID7000C instrument (SONY), with data acquisition performed via ID7000 Software Analysis Mode (SONY), and subsequent analysis carried out using FlowJo v10 (FlowJo LLC).

Histology and immunofluorescence

In the experiment, healthy C57BL/6 mice were each administered 100 μL of vaccine containing 10 μg of TS003 mRNA or an equivalent volume of physiological saline via intravenous injection. Two days post-injection, the lymph nodes were harvested from these mice, cleaned, and embedded in optimal cutting temperature (OCT) compound (SAKURA). The embedded tissues were subsequently frozen at -80°C, sectioned to a thickness of 20 μm using a CM1950 cryostat (Leica), and allowed to air dry for 10 minutes. The tissue sections were fixed in 4% paraformaldehyde (60536ES60, YEASEN) at room temperature for one hour in the dark, followed by three rinses with PBS. The tissue sections were then permeabilized with 0.5% Triton X-100 (DE-0694A, BIODEE) for 1.5 hours at room temperature, followed by three washes with PBS. The sections were blocked with 1% bovine serum albumin (BSA, A8020, Solarbio) at 37°C for 0.5 hours, followed by three additional washes with PBS.

The primary antibodies, including CD11c-AF647 (117312, Biolegend), CD11b-PE (101208, Biolegend), and anti-OVA antibody (sc-65984, Santa Cruz Biotechnology), were incubated overnight at 4°C in the dark. Following three further washes with PBS, the sections were incubated with Alexa Fluor® 488 AffiniPure Rabbit Anti-Mouse IgG (H+L) secondary antibody (33906ES60, YEASEN) at 37°C for one hour in the dark, followed by three additional PBS washes. Mounting medium (8961S, Cell Signaling) was applied to the slides, which were then left to sit in the dark at room temperature for one day. Imaging was conducted using a laser scanning confocal microscope (FV3000RS, Olympus).

For histological analysis, major internal organs (heart, liver, spleen, lungs, and kidneys) from different groups of mice were subjected to paraffin embedding and sectioning. Similarly, tumours from mice in different groups also underwent paraffin embedding and sectioning procedures. Hematoxylin and eosin (H&E) staining was performed according to the manufacturer's instructions using a commercial H&E

staining kit (60524ES60, YEASEN) to observe the cellular arrangement patterns and morphologies within organ sections. Imaging of these stained slides was carried out using the 3DHISTECH slide scanning system (Pannoramic, 3DHISTECH), ensuring detailed visualization and documentation of the histological features.

In vivo cell killing assay in mice

In this experiment, each healthy C57BL/6 mouse was administered a 100 μL vaccine containing 10 μg of mRNA corresponding to their designated group. Five technical replicates were established per group to obtain immunized mice. On day 7, additional healthy C57BL/6 mice were euthanized, and their spleens were harvested. The spleens were washed with 1-2 mL of Dulbecco's phosphate-buffered saline (D-PBS, 60152ES76, YEASEN), minced, and suspended in D-PBS to obtain a single-cell suspension. The suspension was then centrifuged at 625 × g for 5 minutes at 4°C. Next, 2 mL of red blood cell lysis buffer (40401ES60, YEASEN) was added to each spleen sample and incubated at room temperature for 2 minutes. The suspension was then mixed with 3 mL of complete RPMI 1640 medium, passed through a 40-μm cell strainer (CSS013040, BIOFIL), and centrifuged again at 625 × g for 5 minutes at 4°C. The supernatant was discarded, and 24 mL of complete RPMI 1640 medium was added. The cells were evenly divided into two portions.

One portion of 12 mL of the target cells was treated with OVA peptide (IO1310, Solarbio) at a final concentration of 10 μg/mL. The cells were incubated at 37°C for 30 minutes in a water bath, washed twice with D-PBS, pelleted, and resuspended in D-PBS for counting. A total of 5×10^6 target and nontarget cells were required per mouse. Both target and nontarget cells were labeled with carboxyfluorescein succinimidyl ester (CFSE, C34570, Thermo) for 15 minutes at room temperature in the dark. The target cells were resuspended in D-PBS containing 2.5 μM CFSE, while the nontarget cells were resuspended in a solution containing 0.25 μM CFSE. Following two washes with complete RPMI 1640 medium, the cells were centrifuged, resuspended in 100 μL of D-PBS per mouse, combined, and each mouse was inoculated with 200 μL of this mixture.

On day 8, single-cell suspensions of splenic cells were harvested from the immunized mice. The CFSE signals were analyzed in these cells via flow cytometry using an LSR Fortessa instrument (BD Biosciences).

Data acquisition was performed using FACSDIVA Software (BD Biosciences), and data analysis was conducted using FlowJo v10 (FlowJo LLC).

The specific lysis activity (%) was determined via the following formula:

$$\text{Specific lysis activity}(\%) = 100 - \frac{\%\text{CFSE}^{\text{high}} \text{ - immunized}/\%\text{CFSE}^{\text{low}} \text{ - immunized}}{\%\text{CFSE}^{\text{high}} \text{ - control}/\%\text{CFSE}^{\text{low}} \text{ - control}} \times 100$$

In vivo tumour model in mice

In this study, 6- to 8-week-old C57BL/6 mice were subcutaneously injected in the left lower abdomen with 3×10^5 B16F10 cells resuspended in 150 μL of PBS. Prior to injection, the hair in the injection area was shaved. Eight days later, each mouse was administered 100 μL of an mRNA vaccine containing 10 μg of Neo001, Neo001X, Neo002, or Neo003 (TS005); an equimolar mixture of Neo002 and Neo003; or physiological saline as a control, marking day 0. Booster injections at the same dose were administered on days 3 and 7, with five technical replicates established for each group. On day 10, the mice were euthanized via CO_2 asphyxiation. The tumour surface areas were measured using a vernier caliper on days 1, 3, 5, 7, and 10, with the long axis (a) and short axis (b) used to approximate the tumour volume via the formula $V = 4\pi ab^2/3$.

On day 10, tumours, spleens, and lymph nodes were harvested from the mice. The tumours were arranged and photographed using a digital camera. The organs were then mechanically disrupted and filtered through a 40-μm cell strainer (CSS013040, BIOFIL) to obtain single-cell suspensions, which were washed with prechilled PBS (4°C). After centrifugation at 300 × g for 5 minutes at 4°C, red blood cells were lysed using a specific lysis buffer (40401ES60, YEASEN). The cells were further processed and stained with a cocktail of antibodies according to the manufacturer's instructions (the details of the antibodies used are specified in **Table S1**). Following incubation, washing, fixation, and resuspension steps, the cells were analysed using a full-spectrum flow cytometer (LE-ID7000C, SONY), with data acquisition performed via ID7000 Software Analysis Mode (SONY) and subsequent analysis conducted using FlowJo v10 (FlowJo LLC). This comprehensive workflow was designed to evaluate the therapeutic effects of mRNA vaccines on tumour growth and immune responses in treated mice.

In vivo melanoma lung metastasis model in mice

In this study, 6- to 8-week-old C57BL/6 mice were intravenously injected via the tail vein with a 100 μL suspension containing 1×10^6 B16F10 cells in PBS on day 1. On days 4 and 8, the mice in each group were administered 100 μL of an mRNA vaccine containing 10 μg of Neo001, Neo001X, Neo002, or Neo003; an equimolar mixture of Neo002 and Neo003; or 100 μL of physiological saline as a control. On day 18, the lungs were carefully harvested from the mice to assess melanoma metastasis. The harvested lungs were gently rinsed with PBS to remove residual blood and then placed in a 60 mm cell culture dish (TCD010060, BIOFIL) containing sufficient PBS to preserve their original structure without distorting the visualization of potential tumours. The lungs were organized by group and photographed using a digital camera to document the extent of melanoma nodules visually. The images were subsequently analysed using ImageJ software developed by the National Institutes of Health (NIH).

The percentage of the metastatic area was calculated via the following formula:

$$\text{Meteastatic area percent (\%)} = \frac{\text{Area of black part}}{\text{Area of total lung}} \times 100$$

Supporting Figures

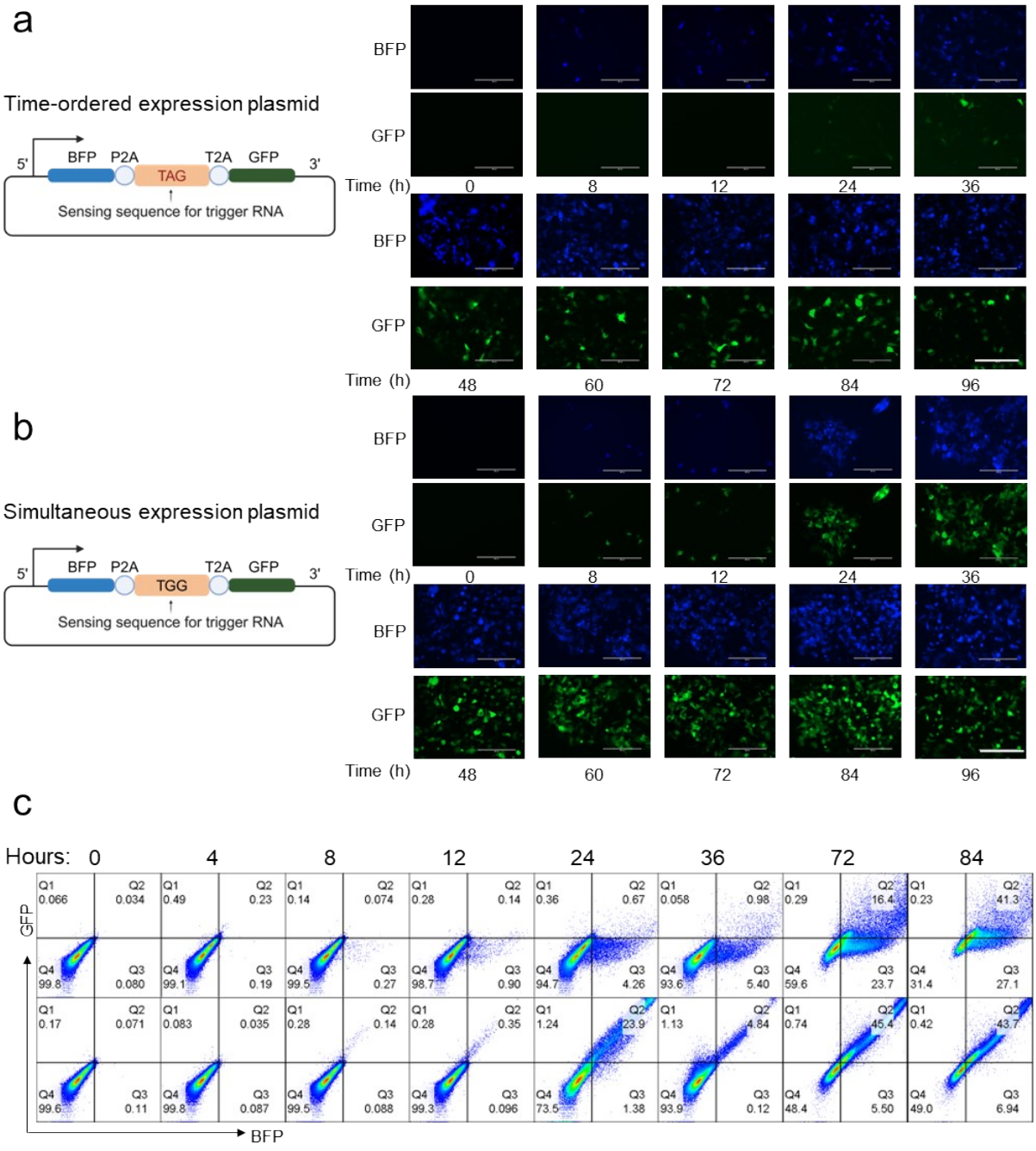

Figure S1: Fluorescence imaging analysis and flow cytometry analysis of the time-ordered expression strategy. a, HEK293FT cells were transfected with time-ordered expression BFP-GFP plasmids. **b,** HEK293FT cells were transfected with simultaneous expression BFP-GFP plasmids. Scale bar, 200 μm. Imaging experiments were repeated three times with independent biological replicates, and representative images are shown. **c,** Fluorescent protein expression levels at different time points after the transfection of

HEK293FT cells with BFP-GFP plasmids. The numbers indicate the percentage of cells in each quadrant. The upper panel shows the percentage of cells transfected with plasmids for time-ordered expression of BFP/GFP, while the lower panel shows the percentage of those transfected with plasmids for simultaneous expression of BFP/GFP. The experiments were repeated three times independently, and representative images are shown.

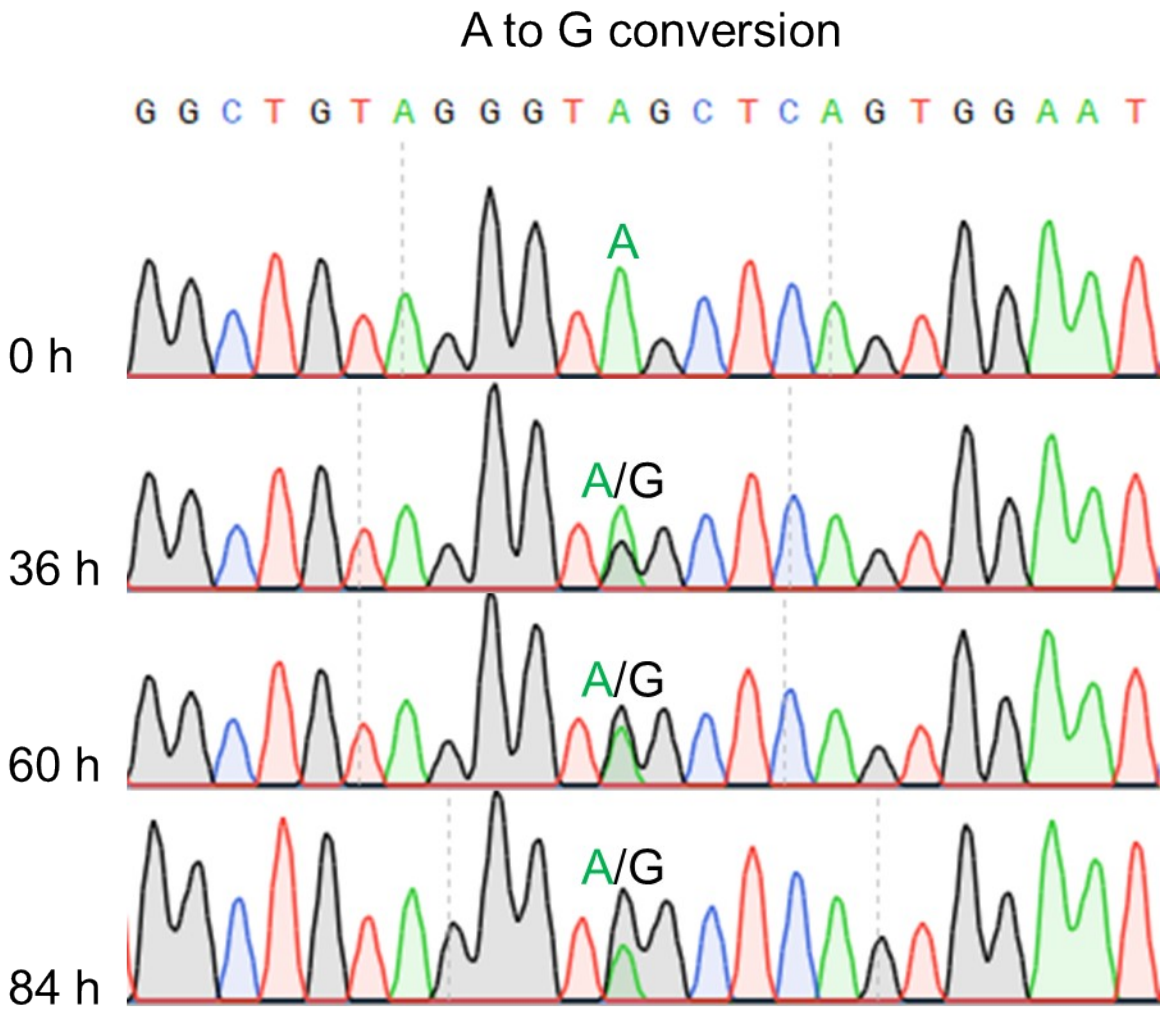

Figure S2: Electropherograms of Sanger sequencing showing A-to-G base conversion at the intended editing site at different time points post-transfection with the time-ordered expression plasmid.

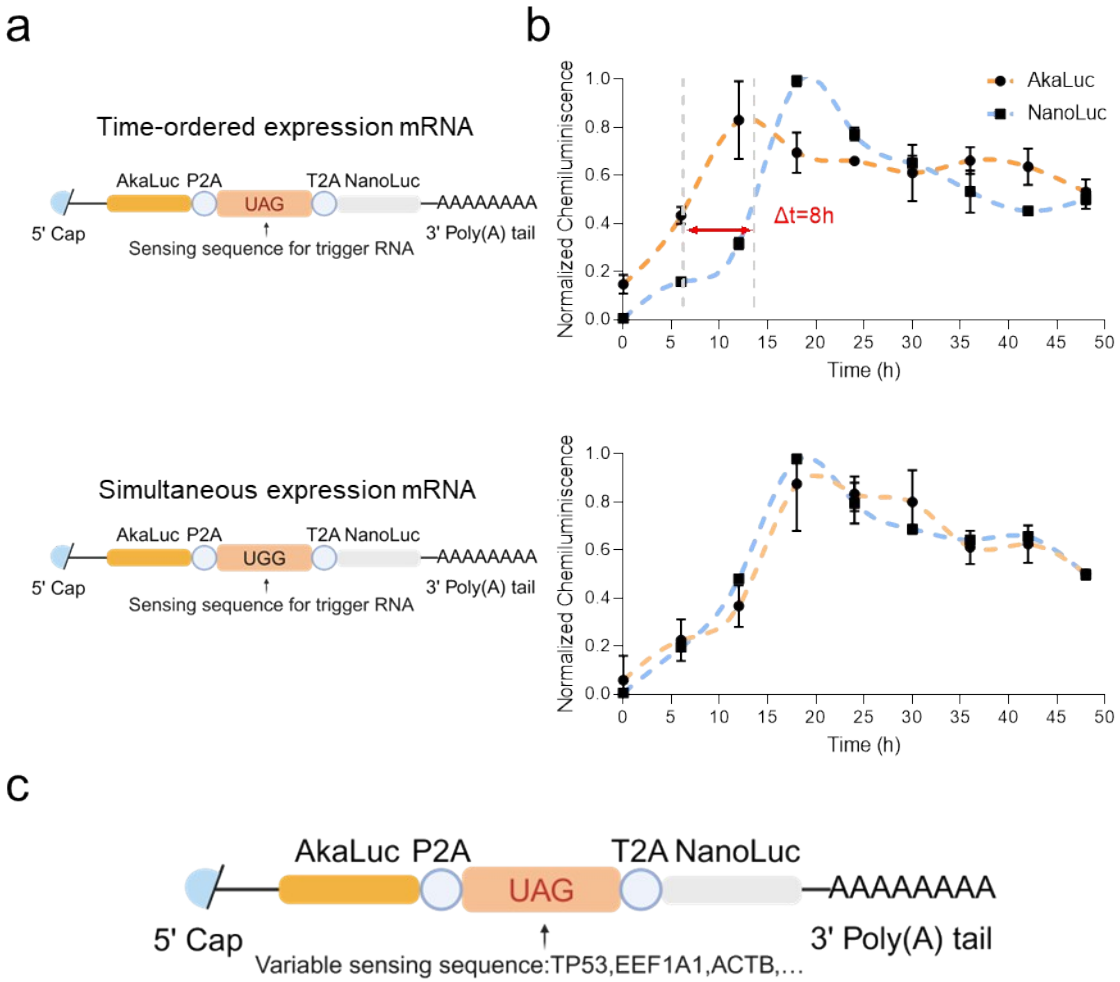

Figure S3: Evaluation of the TOE-mRNA by luciferase expression. a, The AkaLuc-NanoLuc luciferase mRNA reporter system. In the control, the UAG codon was replaced with UGG to simulate 100% editing efficiency (bottom panel). **b,** Chemiluminescence analysis of HEK293FT cells transfected with time-ordered expression (top panel) or simultaneous expression (bottom panel) of AkaLuc-NanoLuc luciferase mRNA. Data are presented as means ± s.d.s from n=3 biologically independent replicate experiments. **c,** Schematic diagram of AkaLuc-NanoLuc TOE-mRNA sequence optimization. Various sensing sequences were designed to target distinct trigger RNAs with different abundances.

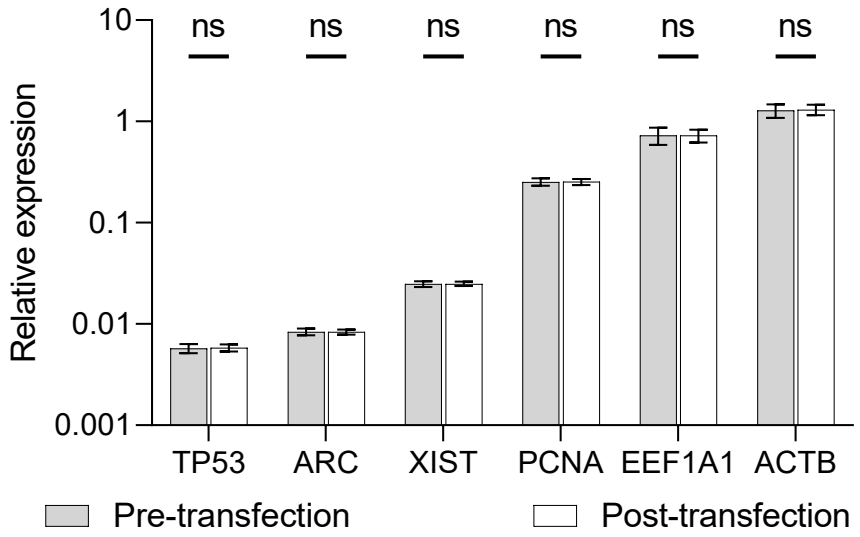

Figure S4: RT-qPCR analysis of relative expression levels of TP53, ARC, XIST, PCNA, EEF1A1, and ACTB in HEK 293FT cells before transfection (Pre-transfection) and 48 h post-transfection with TOE mRNA (Post-transfection), with GAPDH as the reference gene. Data are presented as means ± s.d. (n=3). Statistical significance was assessed by two-way ANOVA with Dunnett's correction. ns, not significant.

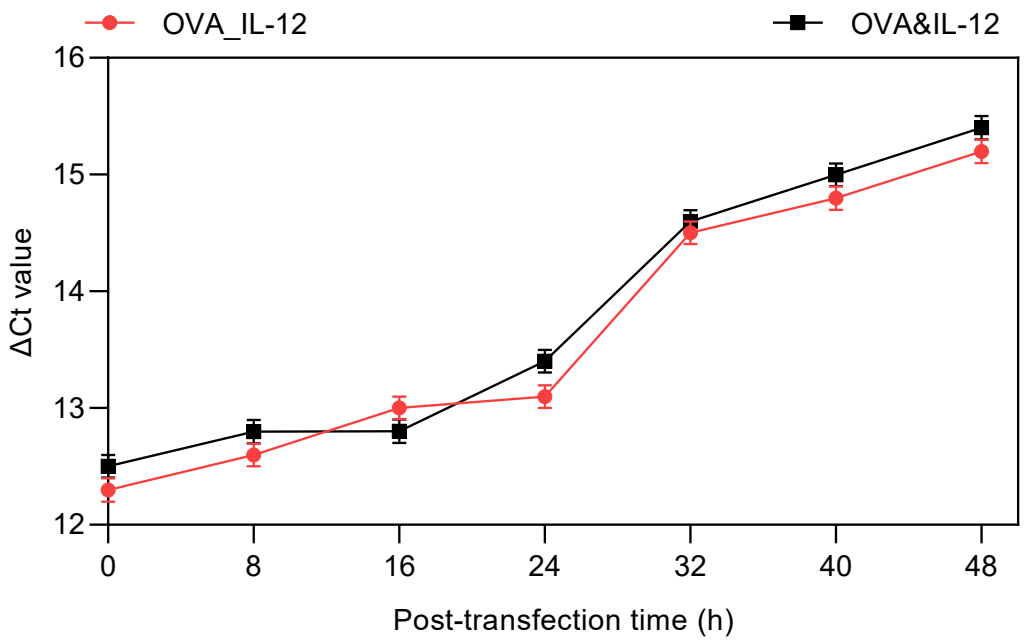

Figure S5: Time-dependent changes in Ct values of TOE mRNA (OVA_IL-12) and simultaneously expressing mRNA (OVA&IL-12) post-transfection. Ct values were determined by qPCR targeting the OVA coding region. Data are presented as mean ± s.d. (n = 3 biologically independent experiments).

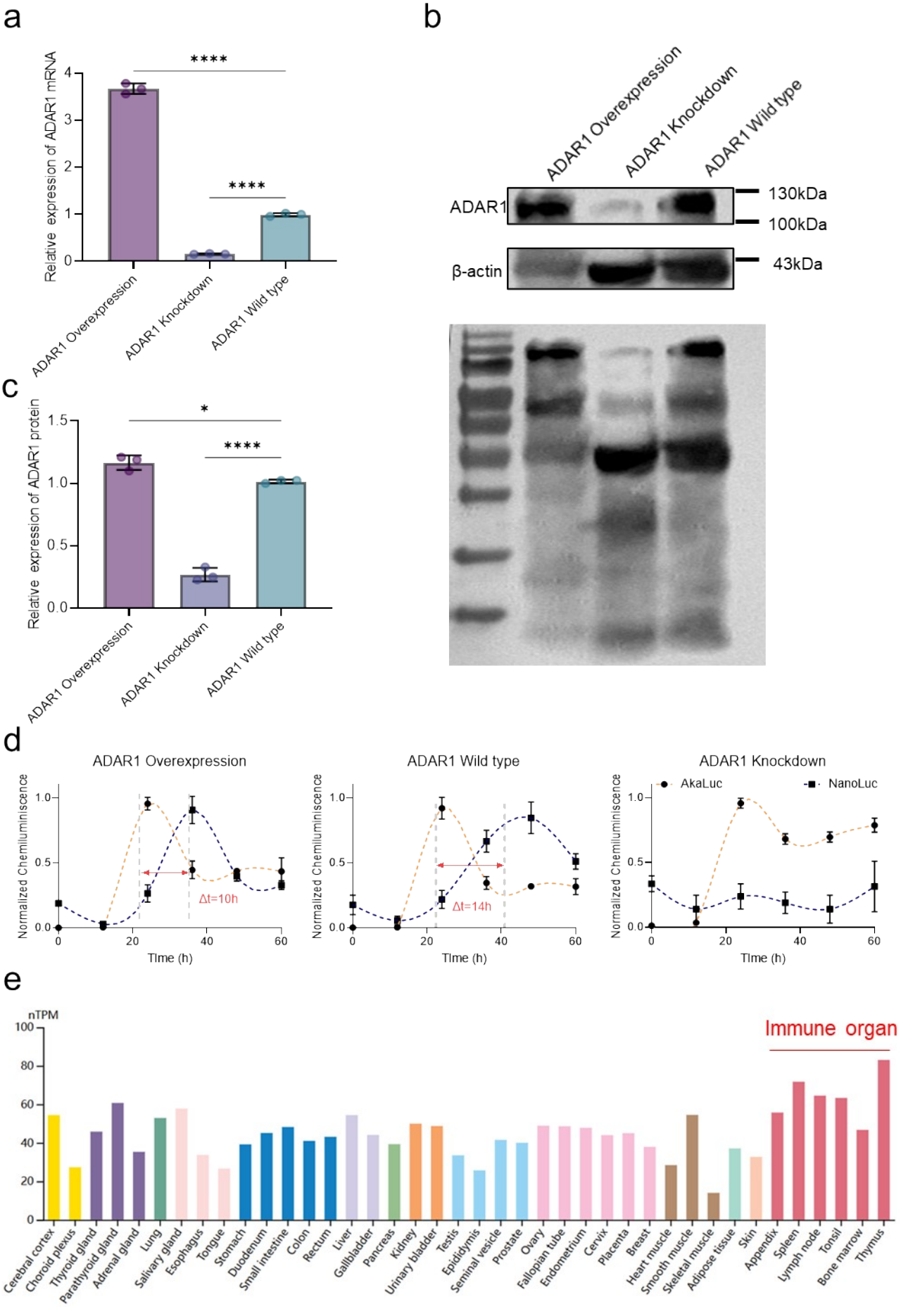
a
Relative expression of ADAR1 mRNA
****
****
ADAR1 Overexpression
ADAR1 Knockdown
ADAR1 Wild type
b
ADAR1 Overexpression
ADAR1 Knockdown
ADAR1 Wild type
ADAR1
130kDa
100kDa
β-actin
43kDa
c
Relative expression of ADAR1 protein
*
****
ADAR1 Overexpression
ADAR1 Knockdown
ADAR1 Wild type
d
ADAR1 Overexpression
ADAR1 Wild type
ADAR1 Knockdown
AkaLuc
NanoLuc
Normalized Chemiluminiscence
Δt=10h
Δt=14h
TIme (h)
e
nTPM
Immune organ
Cerebral cortex
Choroid plexus
Thyroid gland
Parathyroid gland
Adrenal gland
Lung
Salivary gland
Esophagus
Tongue
Stomach
Duodenum
Small intestine
Colon
Rectum
Liver
Gallbladder
Pancreas
Kidney
Urinary bladder
Testis
Epididymis
Seminal vesicle
Prostate
Ovary
Fallopian tube
Endometrium
Cervix
Placenta
Breast
Heart muscle
Smooth muscle
Skeletal muscle
Adipose tissue
Skin
Appendix
Spleen
Lymph node
Tonsil
Bone marrow
Thymus

Figure S6: ADAR1 regulates the expression time of two proteins encoded by TOE-mRNA. a, RT-qPCR analysis of mRNA expression levels of ADAR1 in ADAR1-overexpressing, ADAR1-knockdown, and wild-type HEK293FT cell lines. **b,** Western blot analysis of ADAR1 protein levels in cell lines with three different ADAR1 expression levels. Uncropped scans of the western blots are shown below. **c,** Relative protein expression levels of ADAR1 in these three cell lines, normalized to that of β-actin. **d,** Overexpression or knockdown of ADAR1 resulted in a shortened or extended time difference, respectively, in the expression of the two luciferase proteins. **e,** According to data from The Human Protein Atlas (https://www.proteinatlas.org/), ADAR1 mRNA is highly expressed in immune organs, as indicated in red. The data in **a, c** and **d** are presented as means ± s.d.s from n=3 independent biological experiments, with each data point symbolizing an individual replicate. Statistical significance was assessed by one-way ANOVA with Dunnett's correction. ns, not significant; *P < 0.05; ****P < 0.0001.

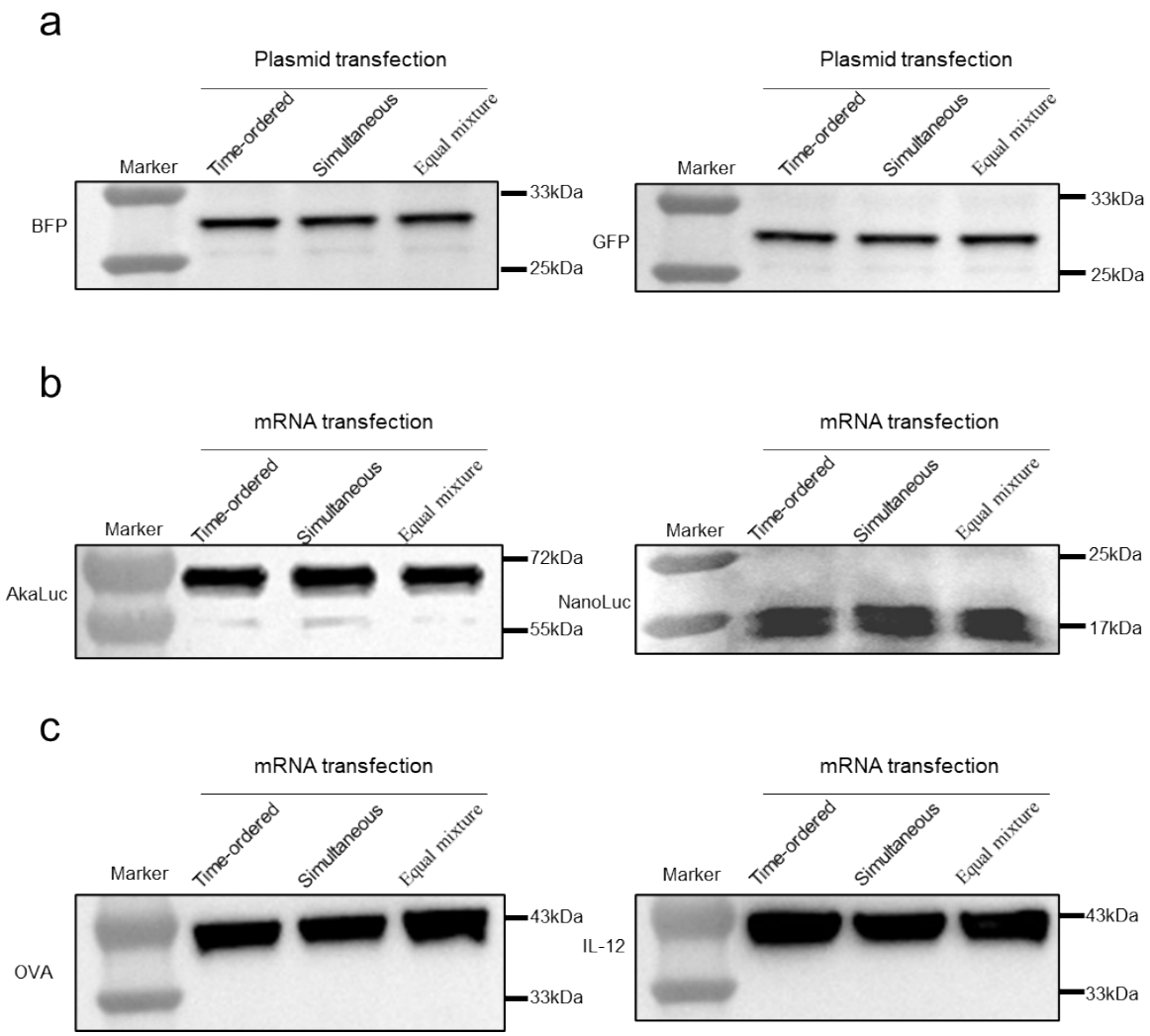

Figure S7: Western blot analysis of the individual protein products in vitro. a, Western blot analysis of BFP and GFP protein levels in HEK293FT cells transfected with three different plasmids. **b,** Western blot analysis of AkaLuc and NanoLuc protein levels in HEK293FT cells transfected with three different mRNAs. **c,** Western blot analysis of OVA and IL-12 protein levels in B16F10 cells transfected with three different mRNAs.

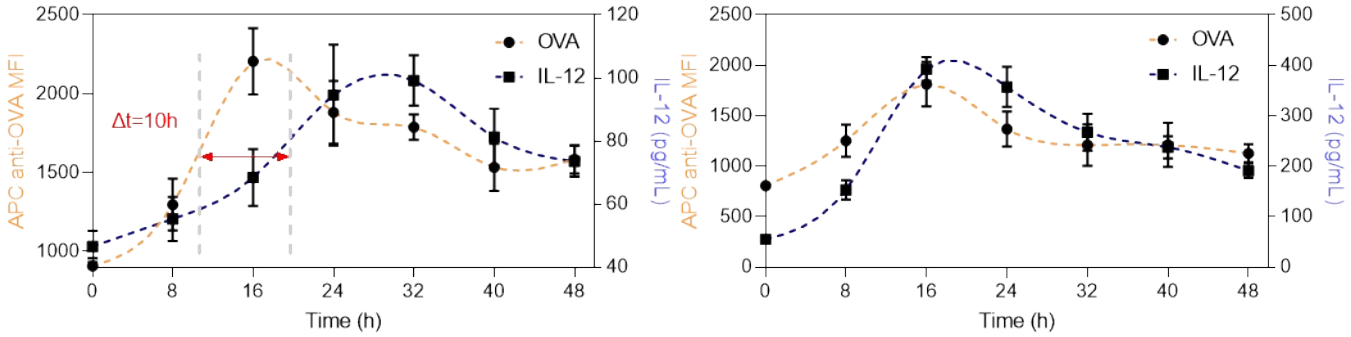

Figure S8: Expression of antigen OVA and adjuvant IL-12 was measured by flow cytometry and ELISA, respectively, after transfection of BMDCs with the TOE mRNA (a) or simultaneously expressed mRNA (b).

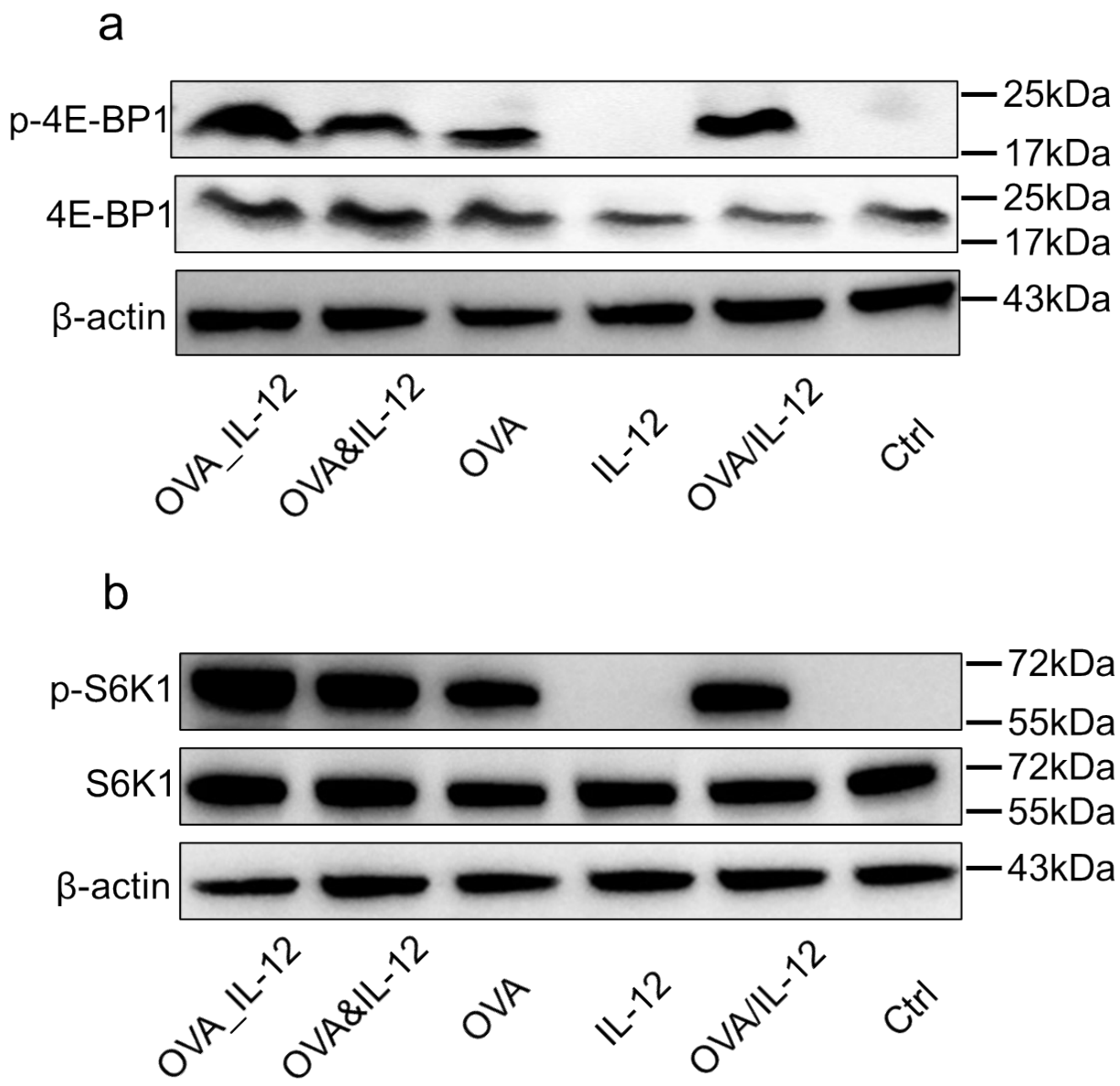

Figure S9: Western blot analysis of phosphorylated key proteins in the mTORC1 pathway. a, Western blot analysis of phosphorylated 4E-BP1.b, Western blot analysis of phosphorylated S6K1.

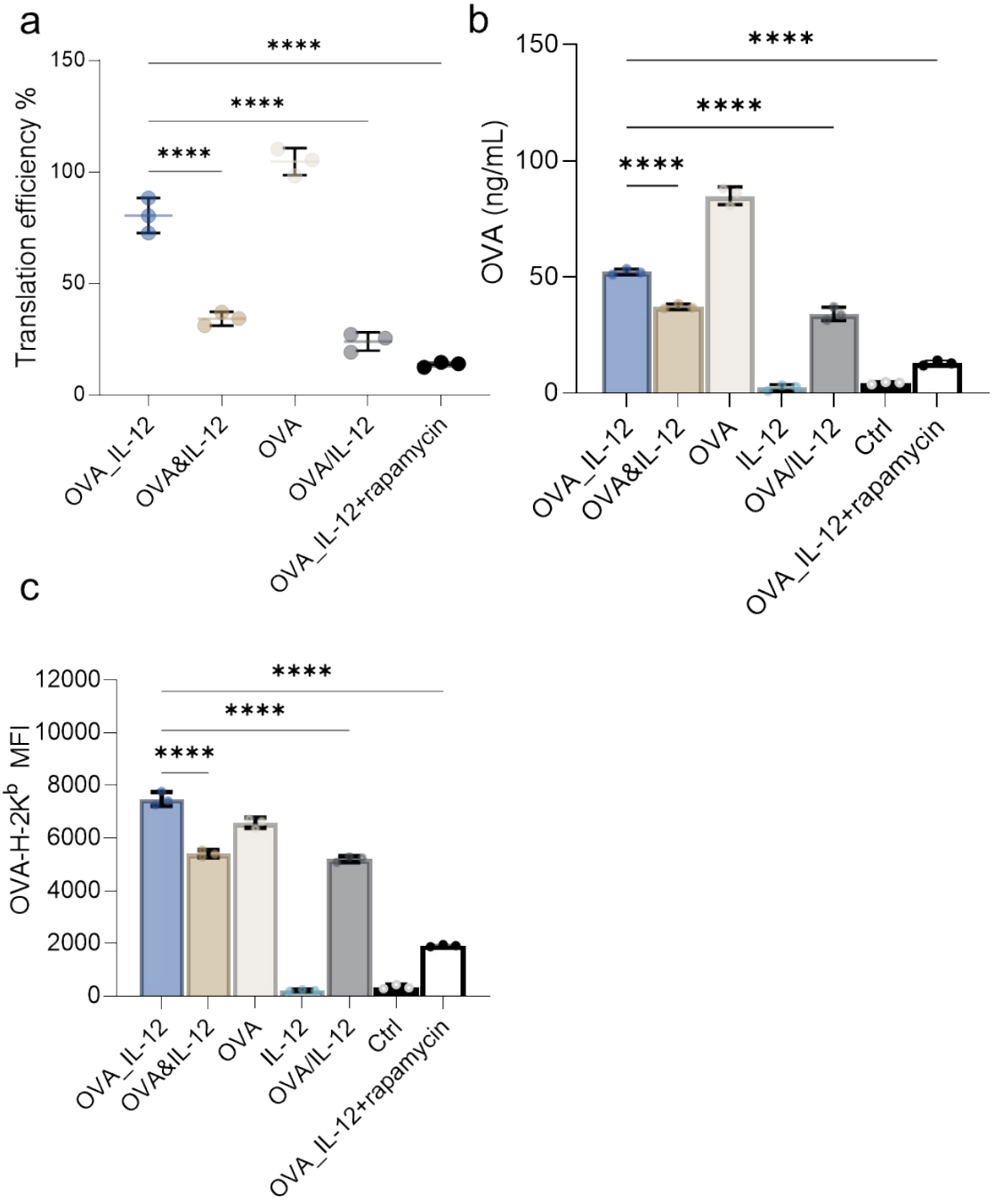

Figure S10: Mechanistic analysis of rapamycin inhibiting TOE mRNA-induced mTORC1 pathway activation a, Ribosome profiling-based qPCR (ribo-qPCR) analysis of OVA antigen translation efficiency in different mRNA vaccine groups, with or without rapamycin treatment.**b,** ELISA analysis of OVA concentration in cell culture medium after BMDCs were treated with various formulations for 24 h, with or without rapamycin treatment.**c,** Flow cytometry analysis of SIINFEKL-H-2K^b antigen presentation levels in different groups, with or without rapamycin treatment.

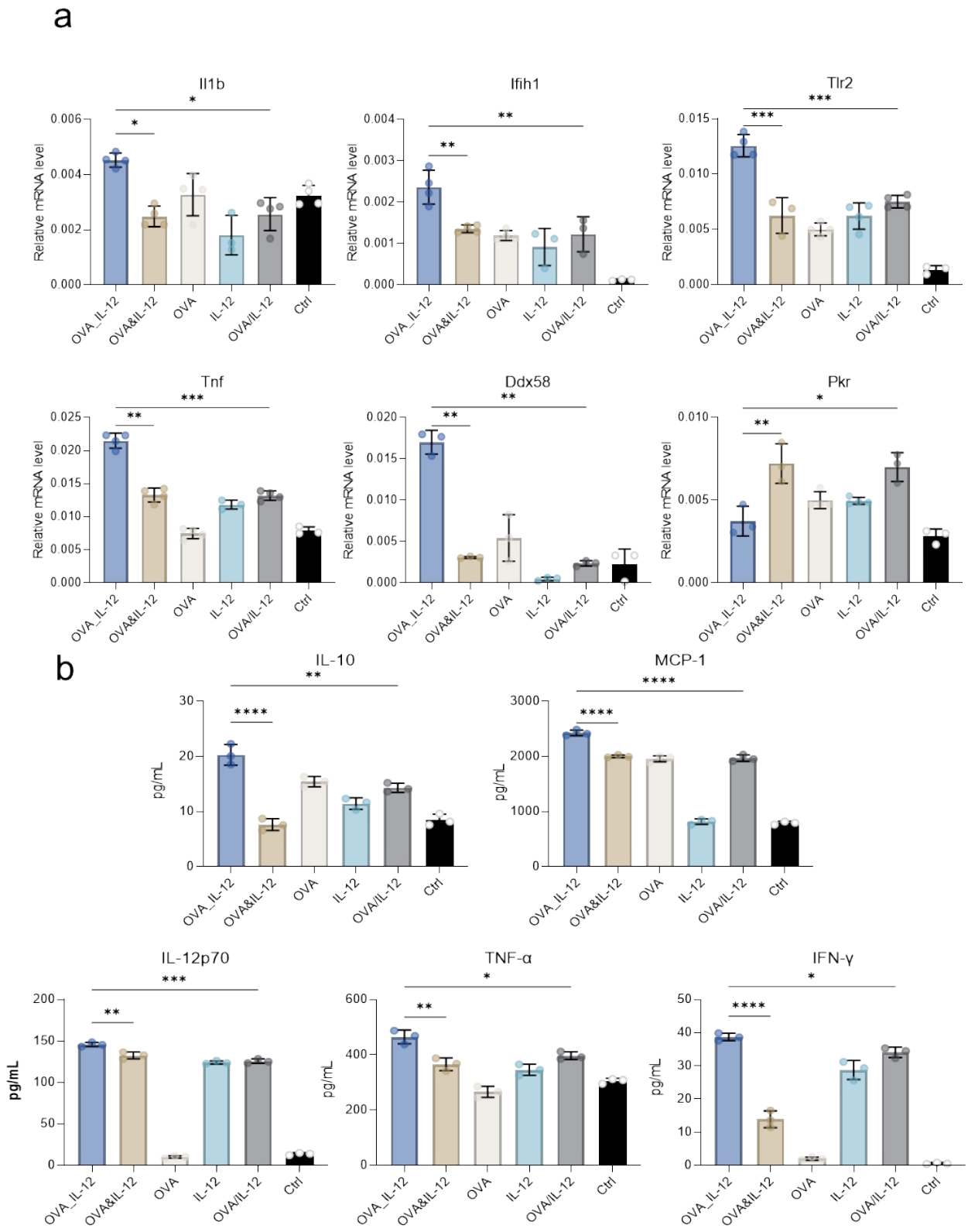

Figure S11: TOE-mRNA activated the immune response of BMDCs. a, RT-qPCR analysis of the gene expression of immune receptors and cytokines in BMDCs 24 h post-transfection with mRNA vaccines. **b,**

Flow cytometric analysis of inflammatory cytokines secretion levels in BMDCs 24 h after mRNA vaccine transfection. The experiments were independently replicated for n=3 biological replicates. Data are presented as means ±s.d.s. Each point represents an individual biological replicate sample. Statistical significance was assessed by one-way ANOVA with Dunnett's correction. ns, not significant; *P < 0.05; **P < 0.01; ***P < 0.001; ****P < 0.0001.

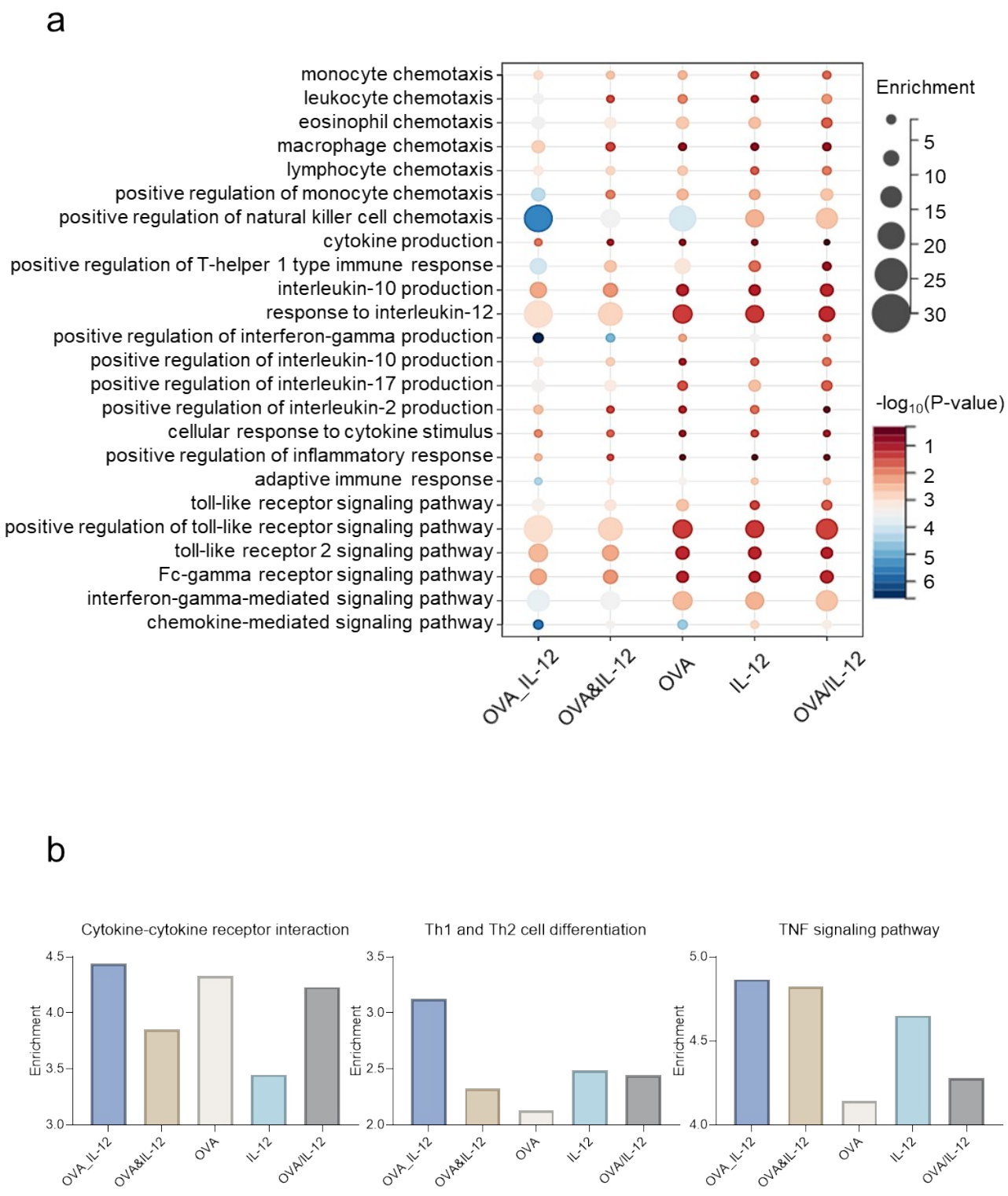

Figure S12: RNA-seq analysis of BMDCs after mRNA vaccine transfection. a, Bubble plot of gene set enrichment analysis results in BMDCs 24 h after mRNA vaccine transfection. **b,** RNA-seq analysis of the enrichment levels of gene sets associated with immune pathways in BMDCs 24 h post-transfection with mRNA.

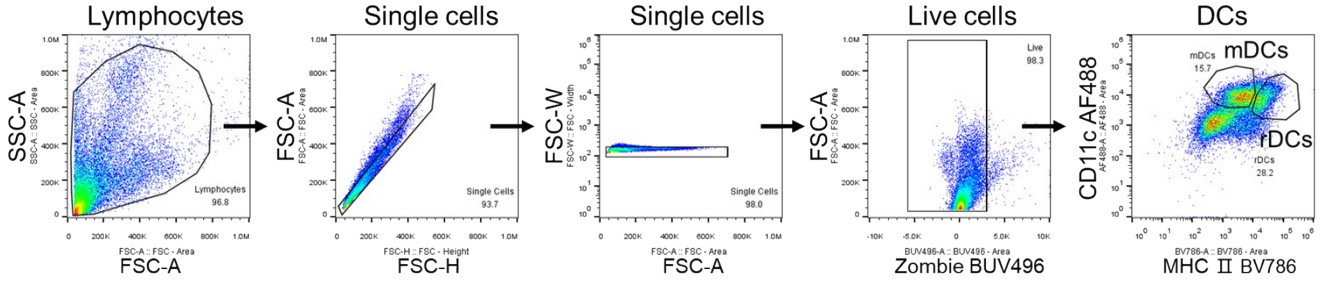

Figure S13: Flow cytometry gating strategy for characterizing BMDC maturation.

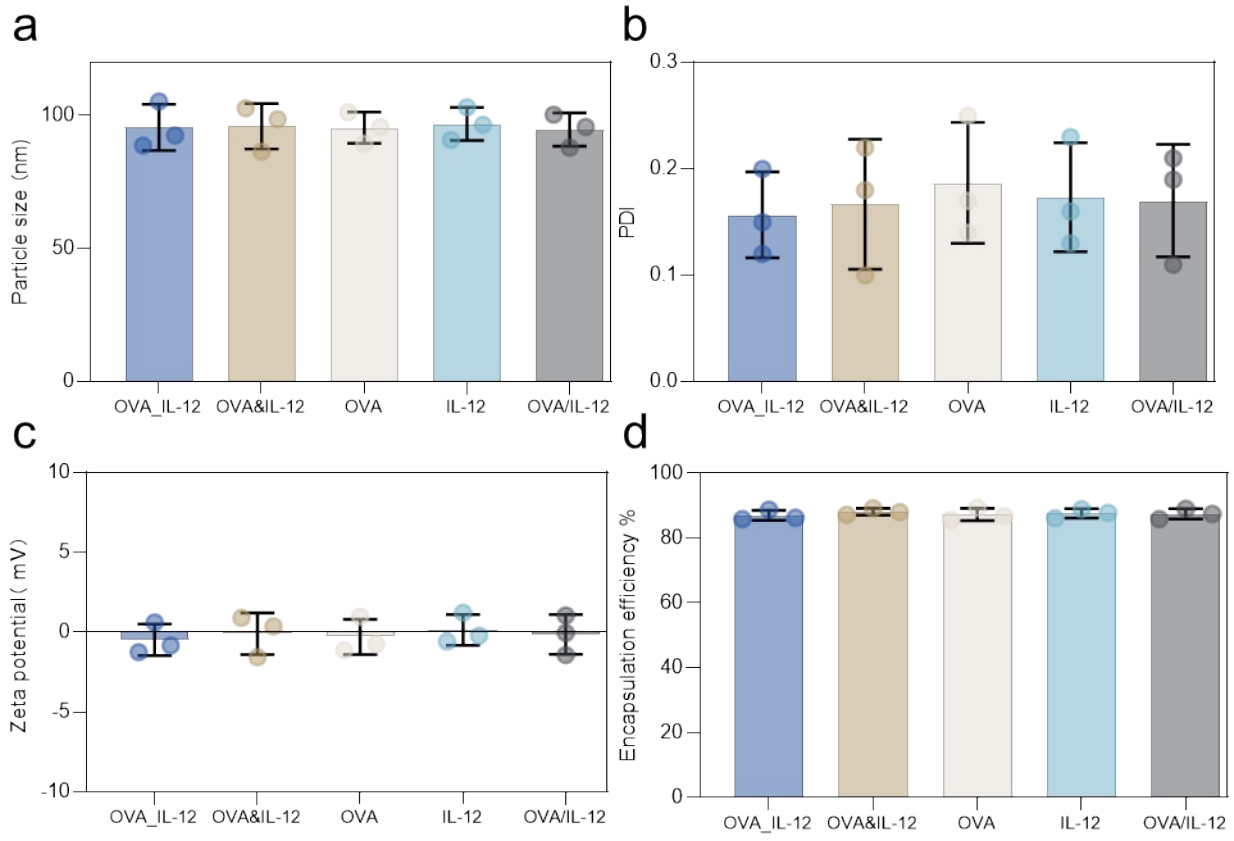

Figure S14: Characterization of LNP-mRNA complexes by physicochemical properties. a, Particle size analysis of LNP-mRNA complexes loaded with distinct mRNA cargos. **b,** Polydispersity index (PDI) evaluation reflecting the size homogeneity of various LNP-mRNA formulations. **c,** Zeta potential measurement indicating the surface charge features of the complexes. **d,** Encapsulation efficiency of mRNA in LNPs determined by quantitative assay. Data are presented as means ± s.d.s from n=3 independent experimental replicates.

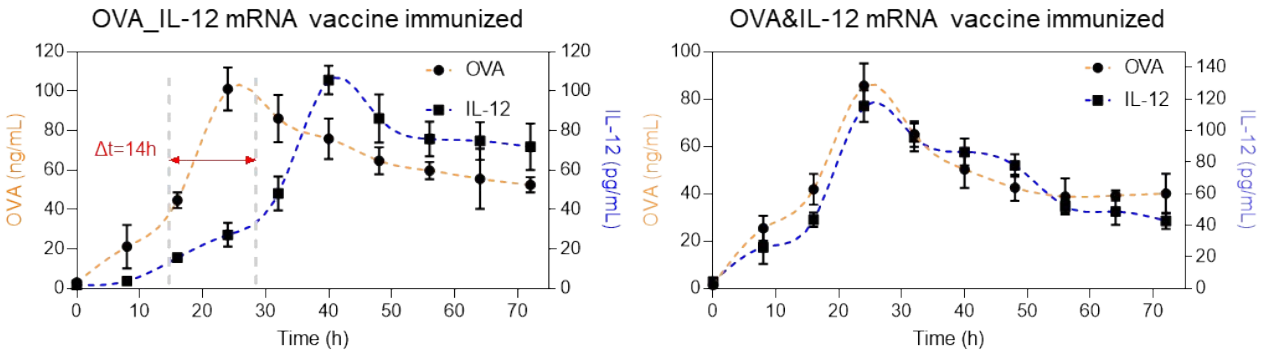

Figure S15: ELISA analysis of OVA and IL-12 in mouse serum for characterizing time-ordered expression in vivo.

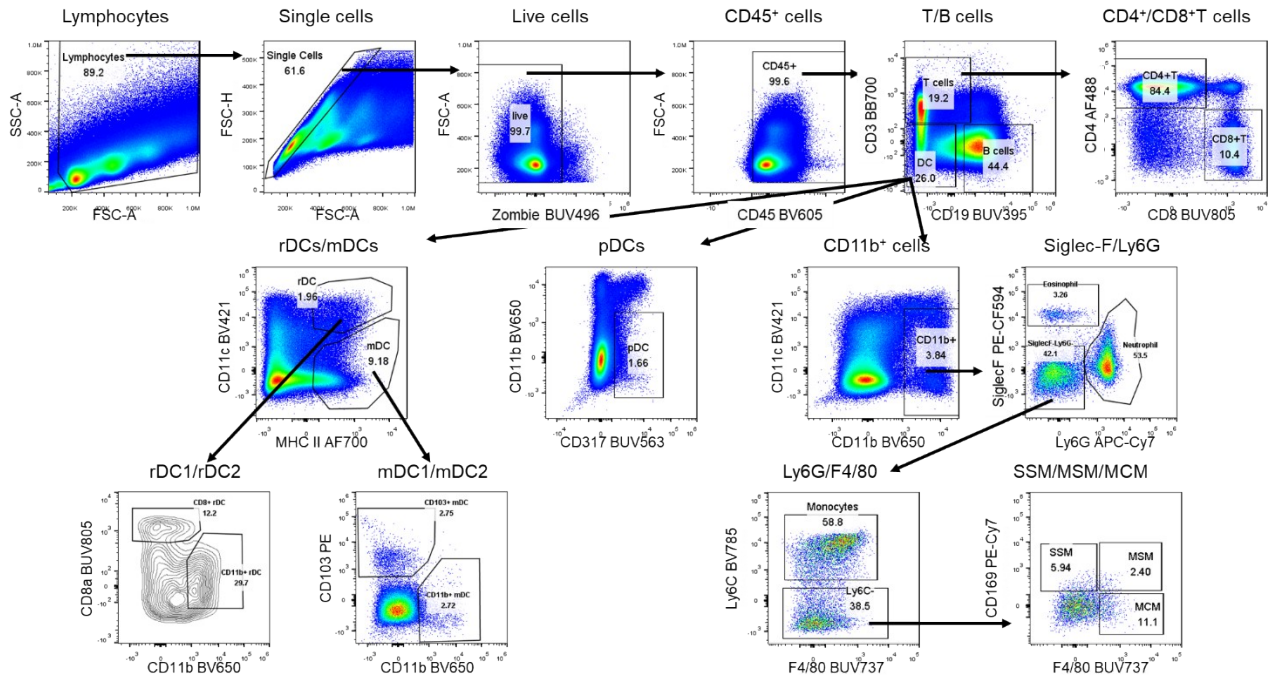

Figure S16: Flow cytometry gating strategy for innate immune cell subset analysis.

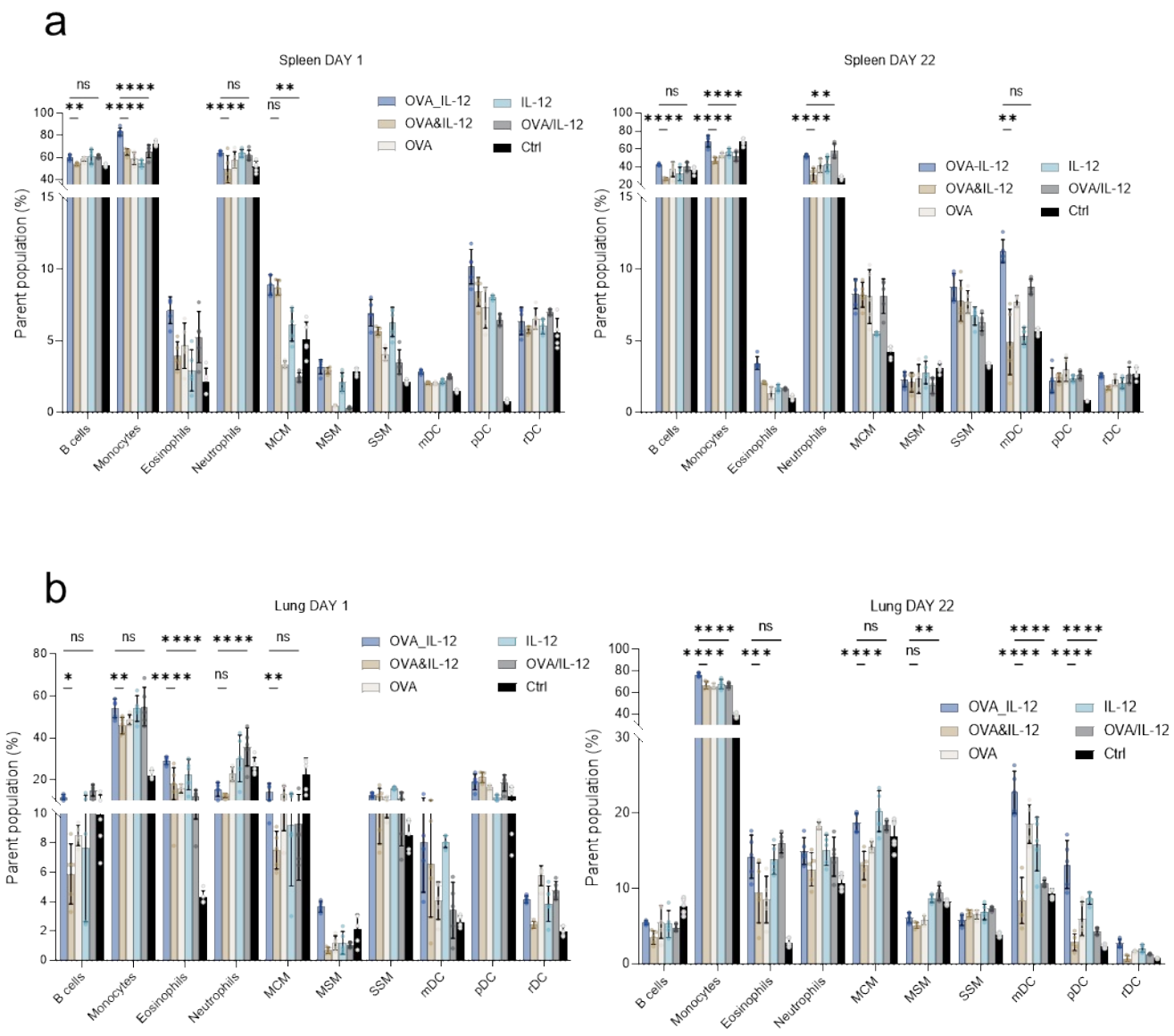

Figure S17: Proportions of different innate immune cell subsets in the spleen (a) and lung (b) after primary (DAY 1) and secondary (DAY 22) immunization. The experiments were independently replicated for n=5 biological replicates. Data are presented as means ±s.d.s. Each point represents an individual biological replicate sample. Statistical significance was assessed by two-way ANOVA with Dunnett's correction. ns, not significant; *P < 0.05; **P < 0.01; ***P < 0.001; ****P < 0.0001.

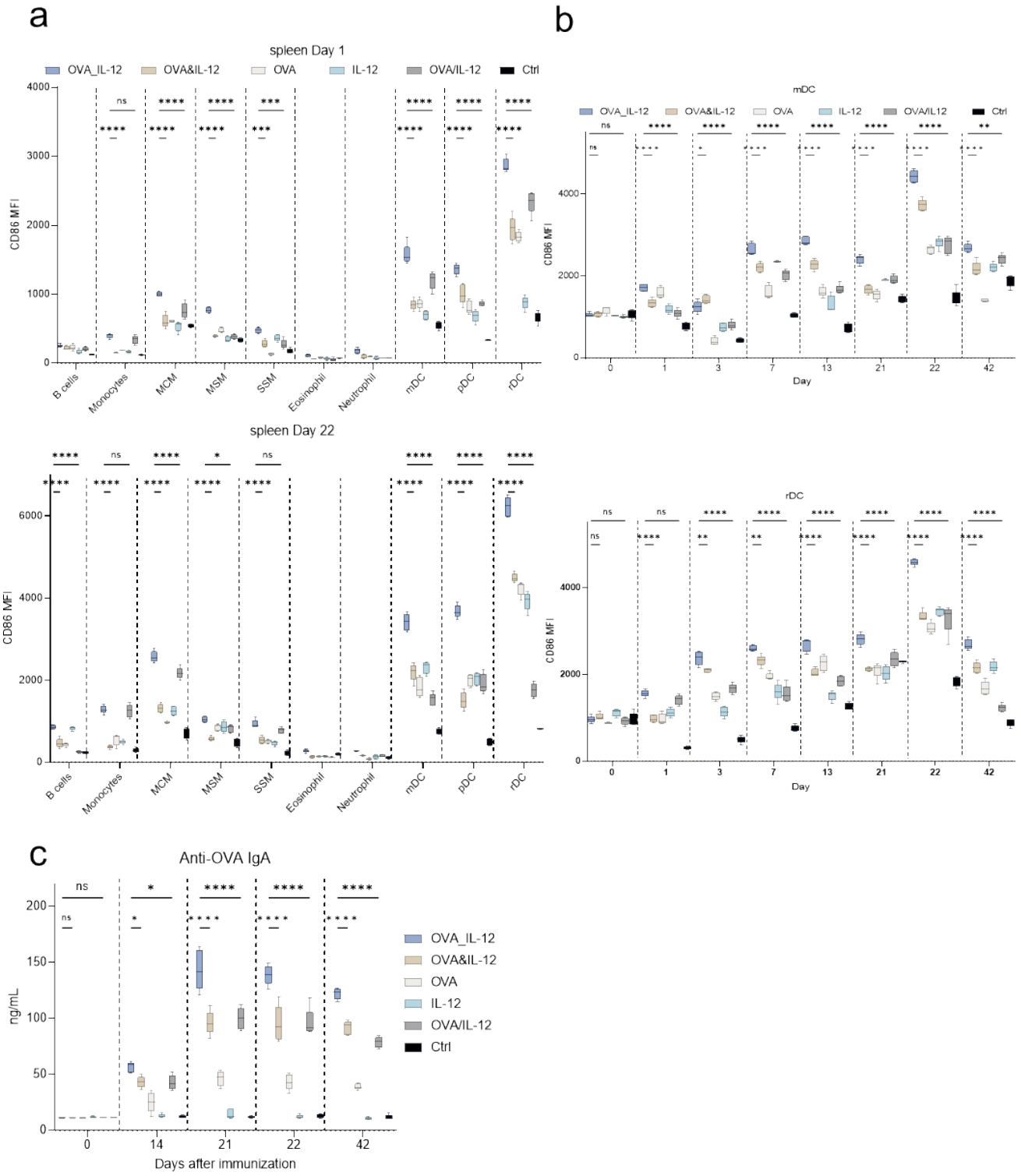

Figure S18: Evaluation of in vivo immune responses in mice injected with different mRNA vaccines. **a,** Expression levels of CD86 on different innate immune cell subsets in the spleen after primary (Day 1) and secondary (Day 22) immunization. **b,** Dynamics of mDC (up) and rDC (bottom) activation in the lymph nodes following mRNA vaccine administration. **c,** ELISA analysis of OVA-specific IgA

antibodies in mouse serum. The experiments were independently replicated for n=5 biological replicates. Data are presented as means ±s.d.s. Each point represents an individual biological replicate sample. Statistical significance was assessed by two-way ANOVA with Dunnett's correction. ns, not significant; *P < 0.05; **P < 0.01; ***P < 0.001; ****P < 0.0001.

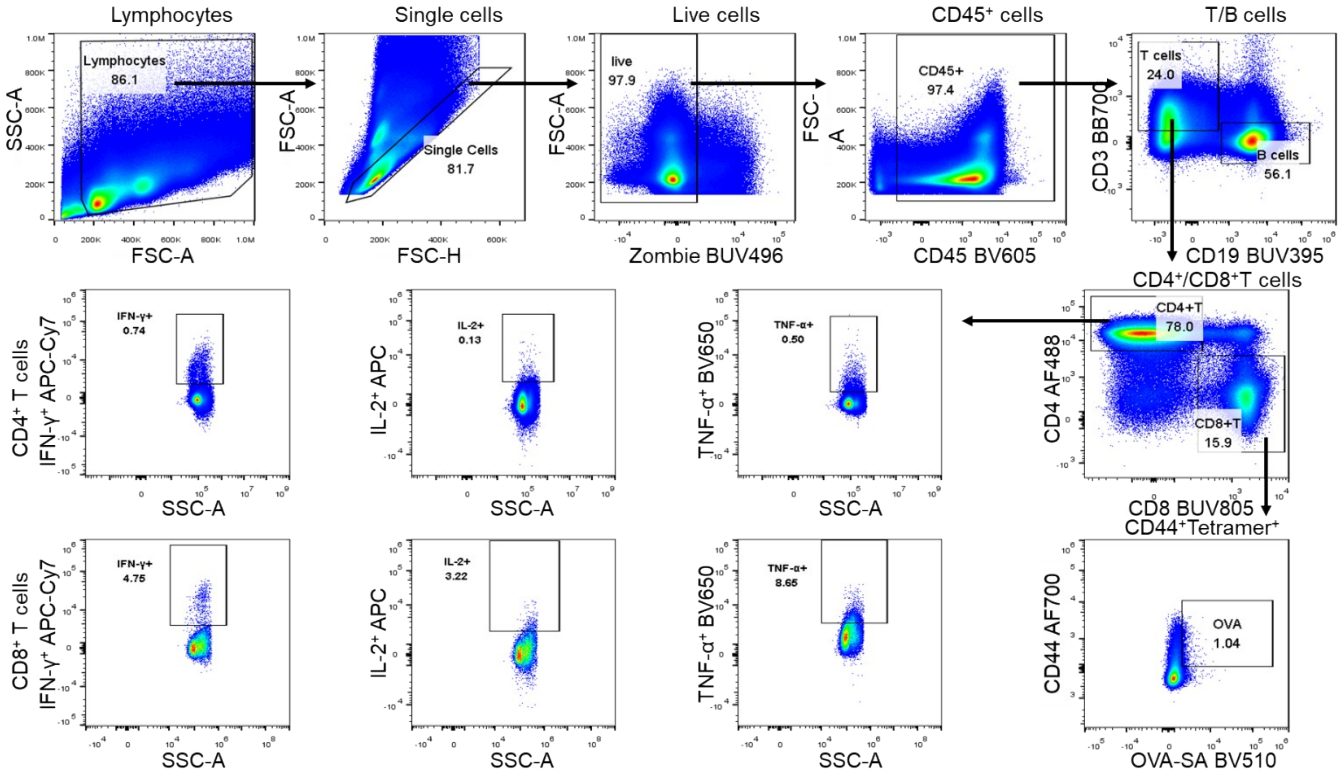

Figure S19: Flow cytometry gating strategy for detecting T-cell cytokine (IFN-γ, IL-2, and TNF-α) expression.

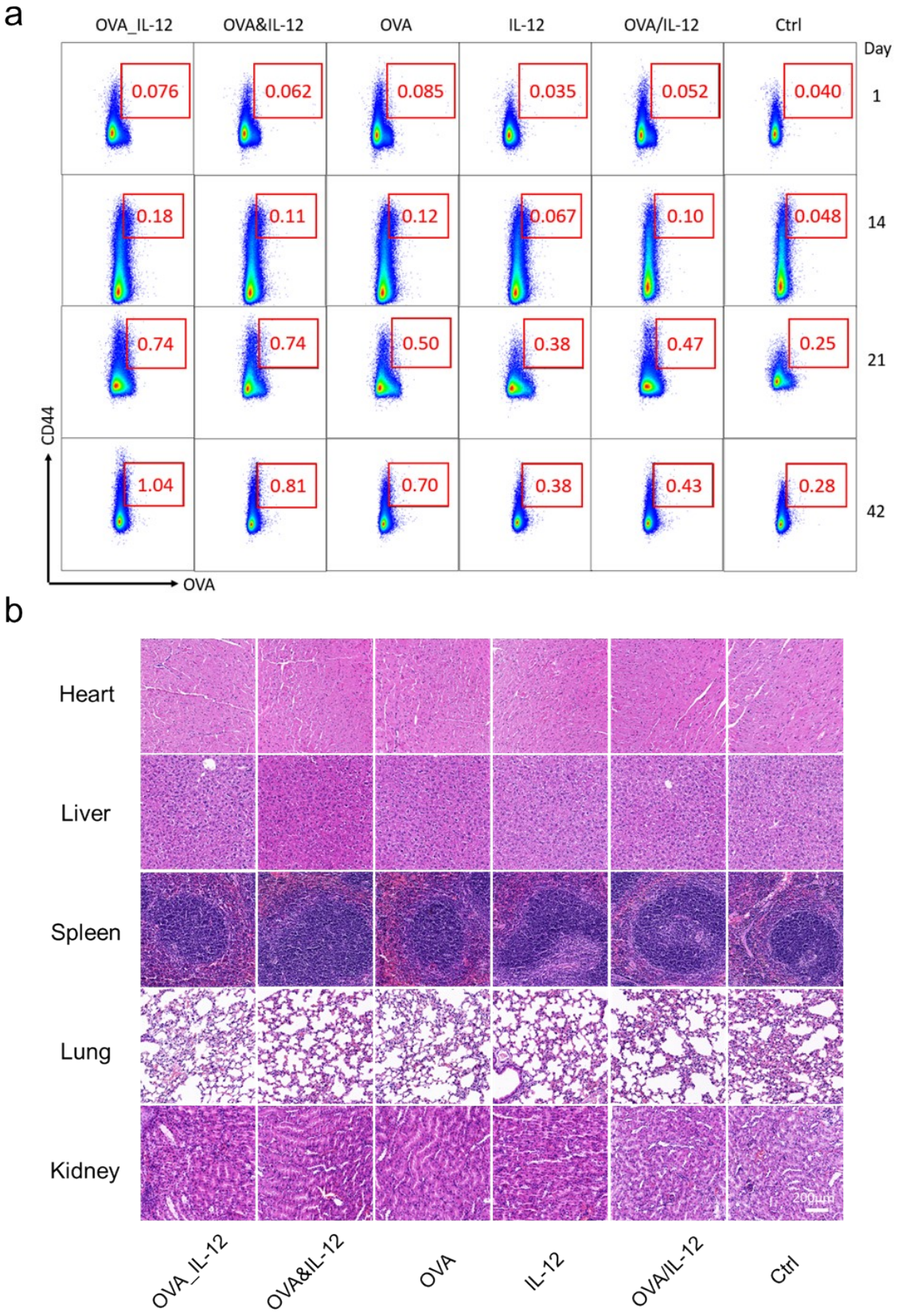

Figure S20: Evaluation of antigen-specific immune responses and the biocompatibility of mRNA

vaccines. **a,** Time-course dynamics of OVA-specific T-cell responses following mRNA vaccine administration. Representative flow cytometry gating results are depicted in the figure. **b,** Representative H&E-stained sections of major organs (heart, kidney, liver, lung, and spleen) from mice after mRNA vaccine administration. n=5 per group. No overt damage was observed. The scale bar represents 200 μm.

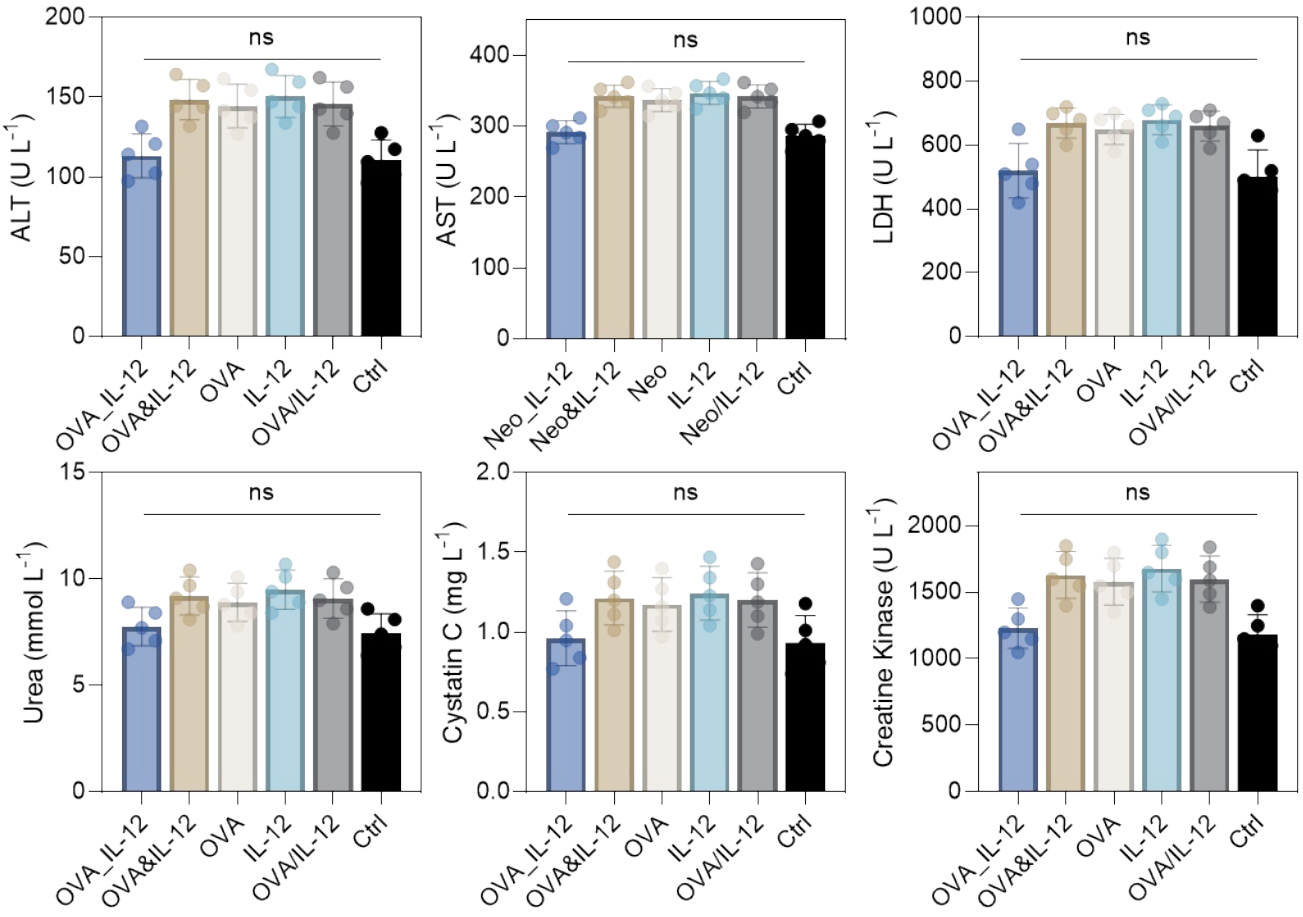

Figure S21: Blood biochemistry and hematology data of mice (n=5). ALT, glutamic-pyruvic transaminase; AST, aspartate aminotransferase; LDH, lactate dehydrogenase; Statistic was based on three mice per data point. Data were mean ± s.d. p values were determined by two-tailed unpaired Student's t-tests. ns represented p>0.05.

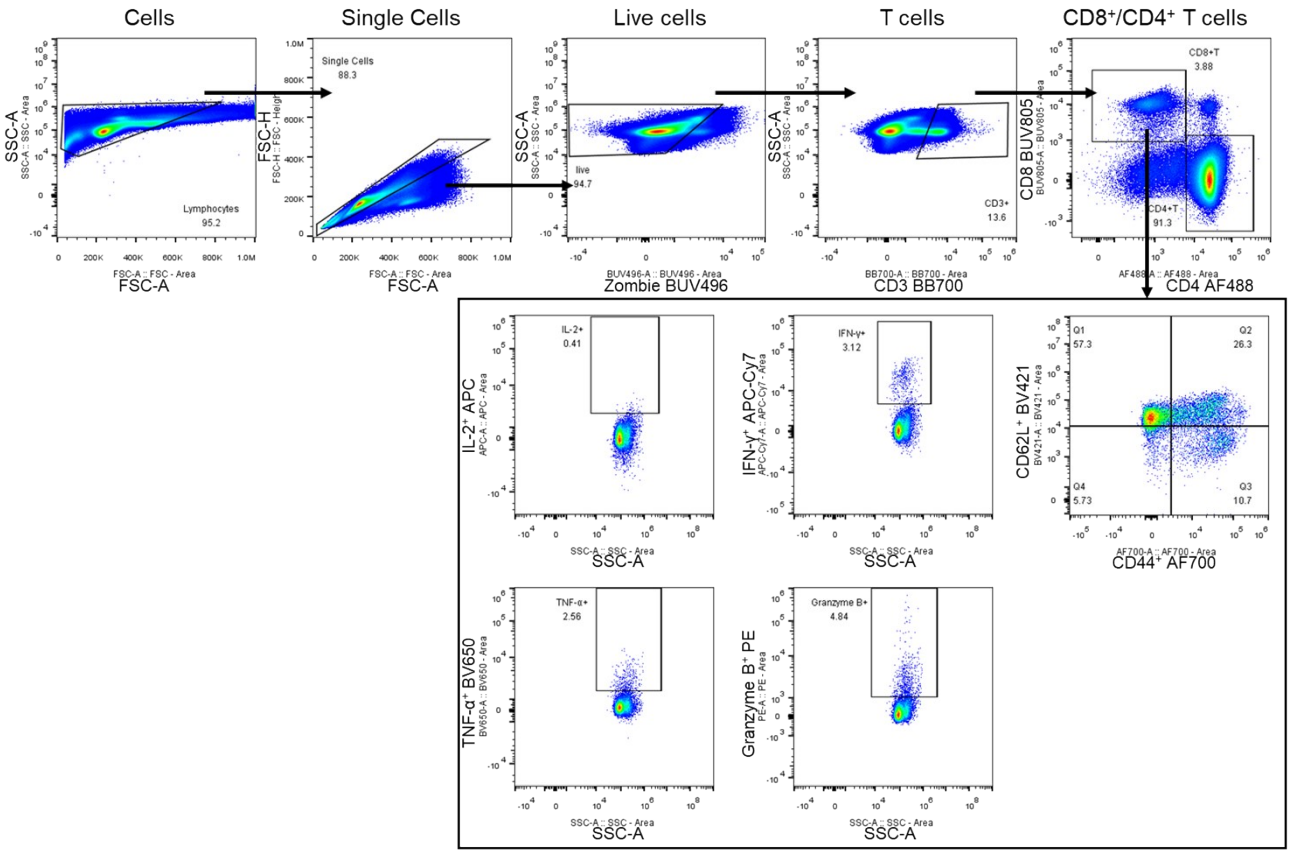

Figure S22: Flow cytometry gating strategy for analysing memory T-cell populations and cytokine expression (IL-2, IFN-γ, TNF-α, and Granzyme B) in the spleens of a mouse melanoma model.

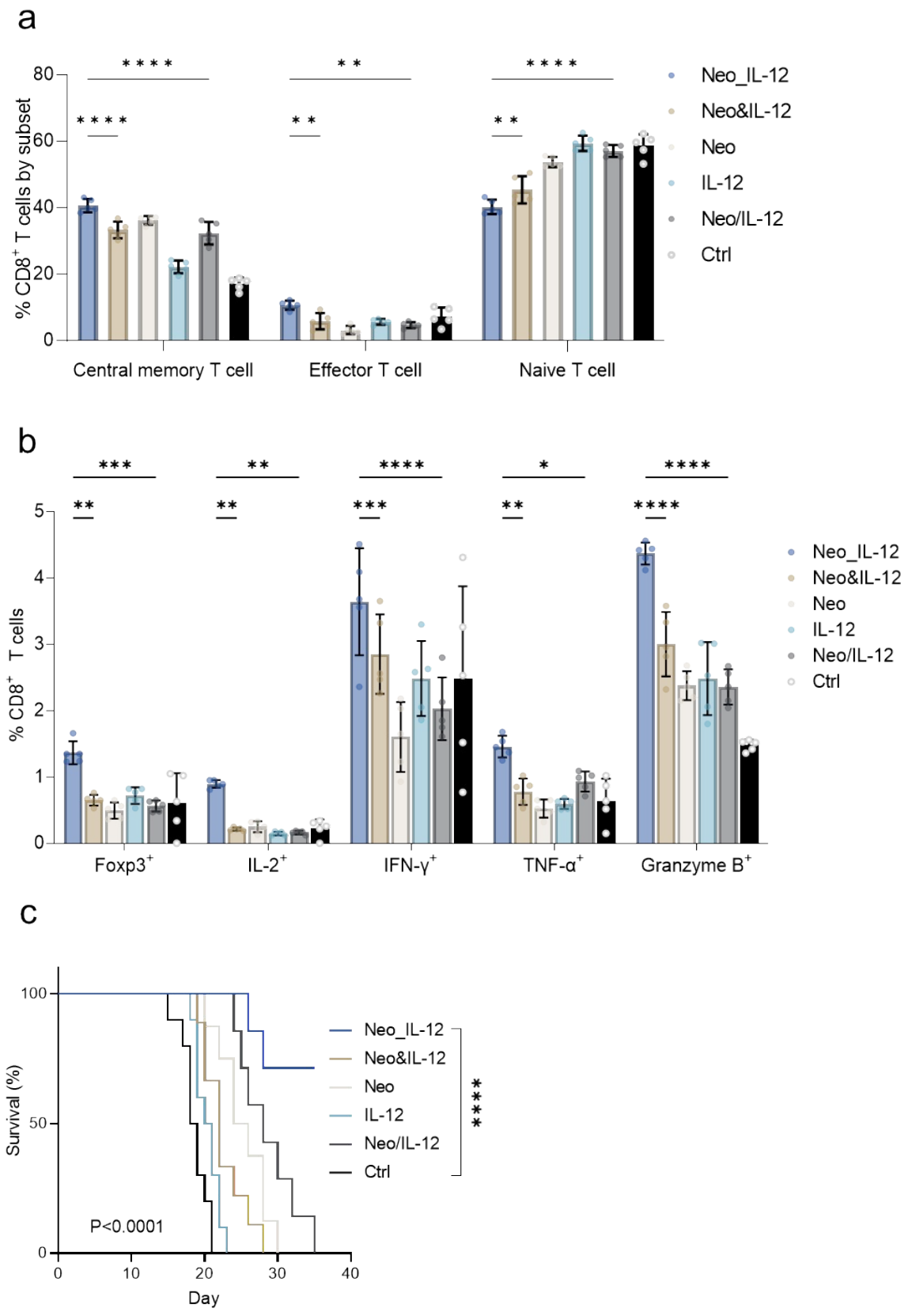

Figure S23: Evaluation of the **cellular immune response and biocompatibility of mRNA vaccines. a,**

Frequencies of naive, effector, and memory $CD8^+$ T-cell subsets within mouse lymph nodes. **b,** Proportions of cytokine-positive cells (IL-2, IFN-γ, TNF-α, and Granzyme B) within mouse lymph nodes. The experiments were independently replicated for n=5 biological replicates. Data are presented as means ±s.d.s, and each point represents an individual biological replicate sample. Statistical significance was assessed by two-way ANOVA with Dunnett's correction. ns, not significant; *P < 0.05; **P < 0.01; ***P < 0.001; ****P < 0.0001. **c,** Survival curves for mice with melanoma lung metastasis (n=10 per group), with statistical significance analysed via the log-rank (Mantel–Cox) test.

Supporting Tables

Table S1 List of multiparameter flow antibodies

BMDC maturation detection

Marker	Fluorophore	Company	Cat#:
Live/Dead	BUV496	Biolegend	423107
OVA-primary	——	Thermo Fisher	13-5743-82
OVA-secondary	BV510	Biolegend	405233
MHC I	PE	Thermo Fisher	12-5958-82
MHC II	BV786	Thermo Fisher	417-5321-82
CD80	BUV737	Thermo Fisher	367-0801-82
CD86	AF647	Biolegend	105019
CD11c	AF488	Thermo Fisher	53-0114-82

Immune model T-cell response detection

Marker	Fluorophore	Company	Cat#:
Live/Dead	BUV496	Biolegend	423107
CD3	BB700	BD Bioscience	742175
CD45	BV605	Biolegend	103139
CD4	AF488	Thermo Fisher	53-0041-82
CD8	BUV805	Thermo Fisher	368-0081-82
CD19	BUV395	Thermo Fisher	363-0193-82
OVA-primary	——	Thermo Fisher	13-5743-82
OVA-secondary	BV510	Biolegend	405233
CD44	AF700	Thermo Fisher	56-0441-82
TNF-α	BV650	Biolegend	506333
IFN-γ	APC-Cy7	Biolegend	505849
IL-2	APC	Thermo Fisher	17-7021-82

Immune model innate immunocyte detection

Marker	Fluorophore	Company	Cat#:
Live/Dead	BUV496	Biolegend	423107
CD3	BB700	BD bioscience	742175
CD45	BV605	Biolegend	103139
CD4	AF488	Thermo Fisher	53-0041-82
CD8a	BUV805	Thermo Fisher	368-0081-82
OVA-primary	——	Thermo Fisher	13-5743-82
OVA-secondary	BV510	Biolegend	405233
CD19	BUV395	Thermo Fisher	363-0193-82
CD11c	BV421	Biolegend	117330
MHC II	AF700	Thermo Fisher	56-5321-82
CD11b	BV650	Biolegend	101239
CD317	BUV563	BD bioscience	749275
CD103	PE	Thermo Fisher	12-1031-82
Siglec-F	PE-CF594	BD bioscience	562757
Ly-6G	APC-Cy7	Biolegend	127623
Ly-6C	BV785	Biolegend	128041
F4/80	BUV737	Biolegend	749283
CD169	PE-Cy7	Biolegend	142412
CD86	AF647	Biolegend	105019

Melanoma model detection

Marker	Fluorophore	Company	Cat#:
Live/Dead	BUV496	Biolegend	423107
CD3	BB700	BD bioscience	742175
CD8a	BUV805	Thermo Fisher	368-0081-82
CD4	AF488	Thermo Fisher	53-0041-82
CD44	AF700	Thermo Fisher	56-0441-82
CD62L	BV421	Thermo Fisher	404-0621-82
TNF-α	BV650	Biolegend	506333
IFN-γ	APC-Cy7	Biolegend	505849
IL-2	APC	Thermo Fisher	17-7021-82
Granzyme B	PE	Thermo Fisher	12-8898-80

Table S2 Key chemical reagents, animals and cells used in this study.

Chemicals, peptides and proteins	SOURCE	IDENTIFIER
FBS	YEASEN	40130ES76
NEAA	YEASEN	60707ES60
GlutaMAX™	Thermo Fisher	35050061
Penicillin–Streptomycin	YEASEN	60162ES76
DMEM without sodium pyruvate	Thermo Fisher	C11965092BT
DMEM	Thermo Fisher	C11995500BT
DMSO	Beyotime	ST038
RPMI 1640	Thermo Fisher	C11875500BT
Hieff Trans® Liposomal Transfection Reagent	YEASEN	40802ES03
Hieff Trans® mRNA Transfection Reagent Hieff Trans® mRNA	YEASEN	40809ES03
Opti-MEM™ I Reduced Serum Medium	Thermo Fisher	31985070
Trypsin-EDTA	YEASEN	40127ES60
PBS	YEASEN	41403ES76
Lysis Buffer for WB/IP Assays	YEASEN	20118ES60
PMSF	BIORIGIN	BN20393
AkaLumine hydrochloride	MCE	HY-112641A
Na_3PO_4	BIORIGIN	BN24319
EDTA	Thermo Fisher	AM9260G
KCl	FeiMoBio	FB9997-500
DTT	INALCO	1758-9030
NP-40	YEASEN	20103ES60
Furimazine	AbMole	M10519
AflII	NEB	R0520VVIAL
10×rCutSmart buffer	NEB	B6004SVIAL
TIAN gel Purification Kit	TIANGEN	4992984
10×Transcription buffer	YEASEN	10618ES90
T7 RNA polymerase	YEASEN	10618ES90
rNTP	NEB	N0466S
Inorganic Pyrophosphatase	YEASEN	10658ES10
N1-Me-Pseudo UTP	YEASEN	10651ES20
Recombinant DNase I	YEASEN	10325ES80
GTP	YEASEN	10132ES03
S-adenosylmethionine (SAM)	YEASEN	10619ES02

Chemicals, peptides and proteins	SOURCE	IDENTIFIER
Murine RNase inhibitor	Vazyme	R301-01
mRNA Vaccinia Capping Enzyme	YEASEN	10614ES84
10× Capping Buffer	YEASEN	10666ES03
mRNA Cap 2′-O-Methyltransferase	YEASEN	10612ES92
Puromycin Dihydrochloride	Beyotime	ST551
Mouse IL-12p70 Elisa Kit	BIORIGIN	BN50536
Mouse IFN-γ Elisa Kit	BIORIGIN	BN50528
Mouse IFN-β(Interferon Beta) ELISA Kit	FineTest	EM1148
Mouse IFN-γ(Interferon Gamma)ELISA Kit	FineTest	EM0093
Mouse IL-2(Interleukin 2) ELISA Kit	FineTest	EM0112
Mouse IL-4(Interleukin 4) ELISA Kit	FineTest	EM0119
Mouse OVA sIgA (Ovalbumin Specific IgA) ELISA Kit	FineTest	EM2036
Mouse OVA sIgG(Ovalbumin Specific IgG) ELISA Kit	FineTest	EM1255
Mouse OVA sIgG1(Ovalbumin Specific IgG1) ELISA Kit	FineTest	EM1996
Mouse OVA sIgG2a(Ovalbumin Specific IgG2a) ELISA Kit	FineTest	EM1997
Ovalbumin (OVA) ELISA Kit	abx259051	Abbexa
RNA Easy Fast Tissue/Cell Kit	TIANGEN	DP451
Hifair® II 1st Strand cDNA Synthesis SuperMix	YEASEN	11119ES60
Hieff® qPCR SYBR Green Master Mix	YEASEN	11201ES03
BCA Protein Quantification Kit	YEASEN	20200ES76
Precast Protein Plus Gel	YEASEN	36248ES10
Enhanced ECL Chemiluminescent Substrate Kit	YEASEN	36222ES76
ADAR1 Antibody	Santa Cruz	sc-73408
Goat Anti-Mouse IgG H&L/HRP Antibody	Bioss	bs-60296G-HRP
β-actin, Rabbit pAb	YEASEN	30102ES60
Goat Anti-Rabbit IgG H&L (HRP) Antibody	Abcam	ab6721
Ovalbumin Antibody	Santa Cruz	sc-65984
Alexa Fluor 647 AffiniPure Goat Anti-Mouse IgG(H+L)	YEASEN	33213ES60
EBFP Mouse mAb	Bioss	bsm-33185M
GFP antibody	MCE	HY-P80141
goat anti-rabbit IgG H&L (HRP) antibody	Abcam	ab6721
anti-firefly luciferase antibody	Abcam	ab181640
Donkey anti-Goat IgG H&L antibody	Abcam	ab216775
Anti-NanoLuc® Monoclonal Antibody	Promega	N700A

IL-12B p40 antibody	Santa Cruz Biotechnology	sc-57258
Peroxidase AffiniPure Goat Anti-Rat IgG (H+L)	YEASEN	33301ES60
Red Blood Cell Lysis Buffer	YEASEN	40401ES60
GM-CSF	YEASEN	91108ES08
IL-4	novoprotein	P07750
TRIzol	BIORIGIN	BN20537
BD™ Cytometric Bead Array (CBA) Mouse Inflammation Kit	BD	552364
BSA	Solarbio	A8020
trypan blue	Beyotime	ST798
CPRG	Glpbio	GC47080
glycine	Solarbio	G8200
$MgCl_2$	leagene	NR0220
β-Hydroxyethylmercaptan	Amresco	M131
CellTrace™ CFSE Cell Proliferation Kit	Thermo Fisher	C34570
SM-102	MCE	HY-134541
4% PFA	YEASEN	60536ES60
Triton X-100	BIODEE	DE-0694A
PE anti-mouse/human CD11b Antibody	Biolegend	101208
Alexa Fluor® 647 anti-mouse CD11c Antibody	Biolegend	117312
Alexa Fluor® 488 AffiniPure Rabbit Anti-Mouse IgG(H+L)	YEASEN	33906ES60
ProLong® Gold Antifade Reagent with DAPI	CST	8961S
D-PBS	YEASEN	60152ES76
OVA peptide	Solarbio	IO1310
Tissue-Tek O.C.T.TM Compound	SAKURA	4583

Animals and cell lines	**SOURCE**
C57BL/6 mouse	Beijing Vital River Laboratory Animal Technology Co., Ltd.
OT-I mouse	Shulaibao (Wuhan) Biotechnology Co., Ltd.
HEK293FT	Cell Resource Center, Peking Union Medical College (PCRC)
B16F10	Cell Resource Center, Peking Union Medical College (PCRC)
B3Z	Qingqi(Shanghai)Biotechnology Development Co., Ltd.

Table S3 RT-qPCR primers

Name	Sequence(5' to 3')	Used in
ARC-F	CAACAGGTAACGGAGCACCA	RT-qPCR for the trigger RNA perturbation
ARC-R	GAACGATGAACCCTGAGCCA	
EEF1A1-F	GGTTTGCCGCCAGAACACAG	
EEF1A1-R	AGTCAGCCTGAGATGTCCCT	
ACTB-F	GGCACCACACCTTCTACAATG	
ACTB-R	ATAGCACAGCCTGGATAGCAA	
PCNA-F	GCCCTGGTTCTGGAGGTAAC	
PCNA-R	CATCCTCGATCTTGGGAGCC	
TP53-F	ACCTATGGAAACTACTTCCTGAAA	
TP53-R	ACCATCGCTATCTGAGCAGC	
XIST-F	CTTGGATGGGTTGCCAGCTA	
XIST-R	TCATGCCCCATCTCCACCTA	
GAPDH-F	GGAGCGAGATCCCTCCAAAAT	
GAPDH-R	GGCTGTTGTCATACTTCTCATGG	
Ddx58-F	AAGAGCCAGAGTGTCAGAATCT	RT-qPCR for immune gene
Ddx58-R	AGCTCCAGTTGGTAATTTCTTGG	
Ifih1-F	AGATCAACACCTGTGGTAACACC	
Ifih1-R	CTCTAGGGCCTCCACGAACA	
Pkr-F	ATGCACGGAGTAGCCATTACG	
Pkr-R	TGACAATCCACCTTGTTTTCGT	
Il1b-F	GCAACTGTTCCTGAACTCAACT	
Il1b-R	ATCTTTTGGGGTCCGTCAACT	
Tlr2-F	GCAAACGCTGTTCTGCTCAG	
Tlr2-R	AGGCGTCTCCCTCTATTGTATT	
Tnf-F	CCCTCACACTCAGATCATCTTCT	
Tnf-R	GCTACGACGTGGGCTACAG	
Gapdh-F	AGGTCGGTGTGAACGGATTTG	
Gapdh-R	TGTAGACCATGTAGTTGAGGTCA	
ADAR1-F	CTGAGACCAAAAGAAACGCAGA	RT-qPCR for ADAR1 regulation
ADAR1-R	GCCATTGTAATGAACAGGTGGTT	
ACTB-F	GGCACCACACCTTCTACAATG	
ACTB-R	ATAGCACAGCCTGGATAGCAA	
Ova-F	GTGCAAAAGACAGCACCAGG	Ribosome RIP-qPCR
Ova-R	CTACTGGCAAGGCTGAACGA	
Actb-F	GGCTGTATTCCCCTCCATCG	
Actb-R	CCAGTTGGTAACAATGCCATGT	

Table S4 Plasmid information

Plasmids	Figure index	Constructs (backbone)	GenBank accession number
pRE001	**Figure 1b-e**	BFP-sensing-GFP	PX095311
pRE001X	**Figure S1, S4a**	BFP-sensingX-GFP	PX095312

Table S5 mRNA information

Plasmids corresponding to mRNA	Figure index	Constructs (backbone)	GenBank accession number
pTS002	**Figure 1f-g**	AkaLuc-sensing-NanoLuc	PX095313
pTS002X	**Figure S2a-c, S4b**	AkaLuc-sensingX-NanoLuc	PX095318
pTS002-ACTB	**Figure 1f-g** **Figure 2c**	AkaLuc-sensing^{ACTB}-NanoLuc	PX095314
pTS002X-ACTB		AkaLuc-sensingX^{ACTB}-NanoLuc	PX095319
pTS002-ARC		AkaLuc-sensing^{ARC}-NanoLuc	PX095315
pTS002X-ARC		AkaLuc-sensingX^{ARC}-NanoLuc	PX095320
pTS002-PCNA		AkaLuc-sensing^{PCNA}-NanoLuc	PX095316
pTS002X-PCNA		AkaLuc-sensingX^{PCNA}-NanoLuc	PX095322
pTS002-TP53		AkaLuc-sensing^{TP53}-NanoLuc	PX095317
pTS002X-TP53		AkaLuc-sensingX^{TP53}-NanoLuc	PX095323
pTS002-XIST		AkaLuc-sensing^{XIST}-NanoLuc	PX095321
pTS002X-XIST		AkaLuc-sensingX^{XIST}-NanoLuc	PX095324
pTS003	**Figure 1h-j** **Figure S4c, S5a**	OVA-sensing-IL-12	PX095325
pTS003X		OVA-sensingX-IL-12	PX095326
pLV-ADAR1p150-Puro	**Figure S3a-d**	ADAR1p150-Puro	PX095329
pTS003	**Figure 2-4** **Figure S5-14**	OVA-sensing-IL-12	PX095325
pTS003X		OVA-sensingX-IL-12	PX095326
pTS004		OVA	PX095327
pTS005		IL-12	PX095328
pNeo001	**Figure 5** **Figure S15**	Neo-sensing-IL-12	PX095308
pNeo001X		Neo-sensingX-IL-12	PX095309
pNeo002		Neo	PX095310
pNeo003		IL-12	PX095328

Table S6 Sequence of OVA-sensing-IL-12 and Neo-sensing-IL-12 mRNA

Name	mRNA sequence (5' to 3')：Protein I-P2A-sensing-T2A-Protein II
OVA-sensing-IL-12 (3673 nt)	Taatacgactcactatagggagacccaagctggctagcacatttgcttctgacacaactgtgttcactagcaacctcaaacagac gccaccatgggctccatcggtgcagcaagcatggaattttgttttgatgtattcaaggagctcaaagtccaccatgccaatgagaa catcttctactgccccattgccatcatgtcagctctagccatggtatacctgggtgcaaaagacagcaccaggacacaaataaata aggttgttcgctttgataaacttccaggattcggagacagtattgaagctcagtgtggcacatctgtaaacgttcactcttcacttaga gacatcctcaaccaaatcaccaaaccaaatgatgtttattcgttcagccttgccagtagactttatgctgaagagagatacccaatc ctgccagaatacttgcagtgtgtgaaggaactgtatagaggaggcttggaacctatcaactttcaaacagctgcagatcaagcca gagagctcatcaattcctgggtagaaagtcagacaaatggaattatcagaaatgtccttcagccaagctccgtggattctcaaact gcaatggttctggttaatgccattgtcttcaaaggactgtgggagaaagcatttaaggatgaagacacacaagcaatgcctttcag agtgactgagcaagaaagcaaacctgtgcagatgatgtaccagattggtttatttagagtggcatcaatggcttctgagaaaatga agatcctggagcttccatttgccagtgggacaatgagcatgttggtgctgttgcctgatgaagtctcaggccttgagcagcttgag agtataatcaactttgaaaaactgactgaatggaccagttctaatgttatggaagagaggaagatcaaagtgtacttacctcgcatg aagatggaggaaaaatacaacctcacatctgtcttaatggctatgggcattactgacgtgtttagctcttcagccaatctgtctggca tctcctcagcagagagcctgaagatatctcaagctgtccatgcagcacatgcagaaatcaatgaagcaggcagagaggtggtag ggtcagcagaggctggagtggatgctgcaagcgtctctgaagaatttagggctgaccatccattcctcttctgtatcaagcacatc gcaaccaacgccgttctcttctttggcagatgtgtttccccctGAATTCGGATCTGGCGCCACCAACTTCT CTCTGCTGAAGCAGGCCGGCGACGTGGAGGAGAACCCAGGCCCAACTAGTgT TAGCACTTGGCTCCAGCATGTTGTCACCATTCCAACCAGAAATTGGCACAAAT GCTACTGTGTCAGGGTTGTAGCCAATTTTCTTAATGTAGGTGCTGACTTCCTT AACGATTTCCTCGTATCTCTTCTGACTGTATGGTAGCTCGGTGGAATCCATTTT GTTGACACCAACAATCAGCTGTTTCACACCCAGGGTGTAAGCCAGAAGAGCA TGCTCGCGGGTCTGCCCGTTCTTGGAGATACCAGCtccGGATCTGGCGAGGGCA GGGGAAGTCTTCTAACATGCGGGGACGTGGAGGAAAATCCCGGCCCCACTAG Tatgtgtcctcagaagctaaccatctcctggtttgccatcgttttgctggtgtctccactcatggccatgtgggagctggagaaaga cgtttatgttgtagaggtggactggactcccgatgcccctggagaaacagtgaacctcacctgtgacacgcctgaagaagatgac atcacctggacctcagaccagagacatggagtcataggctctggaaagaccctgaccatcactgtcaaagagtttctagatgctg

	gccagtacacctgccacaaaggaggcgagactctgagccactcacatctgctgctccacaagaaggaaaatggaatttggtcca ctgaaattttaaaaaatttcaaaaacaagactttcctgaagtgtgaagcaccaaattactccggacggttcacgtgctcatggctggt gcaaagaaacatggacttgaagttcaacatcaagagcagtagcagttcccctgactctcgggcagtgacatgtggaatggcgtct ctgtctgcagagaaggtcacactggaccaaagggactatgagaagtattcagtgtcctgccaggaggatgtcacctgcccaact gccgaggagaccctgcccattgaactggcgttggaagcacggcagcagaataaatatgagaactacagcaccagcttcttcatc agggacatcatcaaaccagacccgcccaagaacttgcagatgaagcctttgaagaactcacaggtggaggtcagctgggagta ccctgactcctggagcactccccattcctacttctccctcaagttctttgttcgaatccagcgcaagaaagaaaagatgaaggaga cagaggaggggtgtaaccagaaaggtgcgttcctcgtagagaagacatctaccgaagtccaatgcaaaggcgggaatgtctgc gtgcaagctcaggatcgctattacaattcctcatgcagcaagtgggcatgtgttccctgcagggtccgatccggcggcggcggg agtggcggcgggggttctggcggaggcctcgctagcggtggctccatggtcagcgttccaacagcctcaccctcggcatccag cagctcctctcagtgccggtccagcatgtgtcaatcacgctacctcctcttttggccacccttgccctcctaaaccacctcagtttg gccagggtcattccagtctctggacctgccaggtgtcttagccagtcccgaaacctgctgaagaccacagatgacatggtgaag acggccagagaaaaactgaaacattattcctgcactgctgaagacatcgatcatgaagacatcacacgggaccaaaccagcac attgaagacctgtttaccactggaactacacaagaacgagagttgcctggctactagagagacttcttccacaacaagagggagc tgcctgcccccacagaagacgtctttgatgatgaccctgtgccttggtagcatctatgaggacttgaagatgtaccagacagagtt ccaggccatcaacgcagcacttcagaatcacaaccatcagcagatcattctagacaagggcatgctggtggccatcgatgagct gatgcagtctctgaatcataatggcgagactctgcgccagaaacctcctgtgggagaagcagacccttacagagtgaaaatgaa gctctgcatcctgcttcacgccttcagcacccgcgtcgtgaccatcaacagggtgatgggctatctgagctccgcctgagtttaaa gctcgctttcttgctgtccaatttctattaaaggttcctttgttccctaagtccaactactaaactgggggatattatgaagggccttga gcatctggattctgcctaataaaaaacatttatttcattgcaaAAAAAAAAAAAAAAAAAAAAAAAAAA AAAAGCATATGACTAAAAAAAAAAAAAAAAAAAAAAAAAAAAAAAA AAAAAAAAAAAAAAAAAAAAAAAAAAAAAAAAAc
Neo-sensing-IL-12 (3508 nt)	Taatacgactcactatagggagacccaagctggctagcacatttgcttctgacacaactgtgttcactagcaacctcaaacagac gccaccatggaaggaattaataatttcaagacgccaaacaaatctgaaaaaaggaaatctgtattatgttccactccatgtgtaaat atccctgcctctccatttatgcagaagcttggctttgggactggggtcagcgtttacctaatgaaaagatctccaagagggttgtctc attctccttgggccgtgaaaaagataagtcttttatgcgatgatcattatcgaactgtgtatcagaagagactaactgatgaagctaa gattttaaaaaaccttaatcacccaaacattataggatatcgtgcttttactgaagccagtgatggtagtctgtgccttgctatggagt

	atggaggtgaaaagtctctgaatgacttaatagaagagcggaacaaagacagtggaagtccttttccagcagctgtaattctcaga gttgctttgcacatggccagagggctaaagtacctgcaccaagaaaagaagctgcttcatggagacataaagtcttcaaatgttgt aattaaaggtgattttgaaacaattaaaatctgtgatgtaggagtctctctgccattggatgaaaatatgactgtgactgatcctgagg cctgttatattggtactgagccatggaaacccaaggaagcgttggaagaaaatggcatcattactgacaaggcagatgtgtttgctt ttggccttactctgtgggaaatgatgactttatgtattccacacgtcaatcttccagatgatgatgttgatgaagatgcaacctttgatg agagtgacttcgatgatgaagcatattatgcagctctggggacaaggccatccatcaacatggaagagctggatgactcctacca gaaggccattgaactcttctgtgtgtgcactaatgaggatcctaaagatcgcccgtctgctgcacacatcgttgaagctttggaact agatggccaatgttgtggtctaagctcaaagcattaaGAATTCGGATCTGGCGCCACCAACTTCTCT CTGCTGAAGCAGGCCGGCGACGTGGAGGAGAACCCAGGCCCAACTAGTgTTA GCACTTGGCTCCAGCATGTTGTCACCATTCCAACCAGAAATTGGCACAAATGC TACTGTGTCAGGGTTGTAGCCAATTTTCTTAATGTAGGTGCTGACTTCCTTAA CGATTTCCTCGTATCTCTTCTGACTGTATGGTAGCTCGGTGGAATCCATTTTGT TGACACCAACAATCAGCTGTTTCACACCCAGGGTGTAAGCCAGAAGAGCATG CTCGCGGGTCTGCCCGTTCTTGGAGATACCAGCtccGGATCTGGCGAGGGCAG GGGAAGTCTTCTAACATGCGGGGACGTGGAGGAAAATCCCGGCCCCACTAGT atgtgtcctcagaagctaaccatctcctggtttgccatcgttttgctggtgtctccactcatggccatgtgggagctggagaaagac gtttatgttgtagaggtggactggactcccgatgcccctggagaaacagtgaacctcacctgtgacacgcctgaagaagatgaca tcacctggacctcagaccagagacatggagtcataggctctggaaagaccctgaccatcactgtcaaagagtttctagatgctgg ccagtacacctgccacaaaggaggcgagactctgagccactcacatctgctgctccacaagaaggaaaatggaatttggtccac tgaaattttaaaaaatttcaaaaacaagactttcctgaagtgtgaagcaccaaattactccggacggttcacgtgctcatggctggtg caaagaaacatggacttgaagttcaacatcaagagcagtagcagttcccctgactctcgggcagtgacatgtggaatggcgtctc tgtctgcagagaaggtcacactggaccaaagggactatgagaagtattcagtgtcctgccaggaggatgtcacctgcccaactg ccgaggagaccctgcccattgaactggcgttggaagcacggcagcagaataaatatgagaactacagcaccagcttcttcatca gggacatcatcaaaccagacccgcccaagaacttgcagatgaagcctttgaagaactcacaggtggaggtcagctgggagtac cctgactcctggagcactccccattcctacttctccctcaagttctttgttcgaatccagcgcaagaaagaaaagatgaaggagac agaggaggggtgtaaccagaaaggtgcgttcctcgtagagaagacatctaccgaagtccaatgcaaaggcgggaatgtctgcg tgcaagctcaggatcgctattacaattcctcatgcagcaagtgggcatgtgttccctgcagggtccgatccggcggcggcgggga gtggcggcgggggttctggcggaggcctcgctagcggtggctccatggtcagcgttccaacagcctcaccctcggcatccagc

	agctcctctcagtgccggtccagcatgtgtcaatcacgctacctcctctttttggccacccttgccctcctaaaccacctcagtttgg ccagggtcattccagtctctggacctgccaggtgtcttagccagtcccgaaacctgctgaagaccacagatgacatggtgaaga cggccagagaaaaactgaaacattattcctgcactgctgaagacatcgatcatgaagacatcacacgggaccaaaccagcacat tgaagacctgtttaccactggaactacacaagaacgagagttgcctggctactagagagacttcttccacaacaagagggagctg cctgcccccacagaagacgtctttgatgatgaccctgtgccttggtagcatctatgaggacttgaagatgtaccagacagagttcc aggccatcaacgcagcacttcagaatcacaaccatcagcagatcattctagacaagggcatgctggtggccatcgatgagctga tgcagtctctgaatcataatggcgagactctgcgccagaaacctcctgtgggagaagcagacccttacagagtgaaaatgaagc tctgcatcctgcttcacgccttcagcacccgcgtcgtgaccatcaacagggtgatgggctatctgagctccgcctgagtttaaagc tcgctttcttgctgtccaatttctattaaaggttcctttgttccctaagtccaactactaaactgggggatattatgaagggccttgagca tctggattctgcctaataaaaaacatttattttcattgcaaAAAAAAAAAAAAAAAAAAAAAAAAAAAA AAGCATATGACTAAAAAAAAAAAAAAAAAAAAAAAAAAAAAAAAAAAA AAAAAAAAAAAAAAAAAAAAAAAAAAAAAAc

OVA-sensing-IL-12 mRNA (3673 nt) backbone: OVA-P2A-sensing-T2A-IL-12

Neo-sensing-IL-12 mRNA (3508 nt) backbone: Neo-P2A-sensing-T2A-IL-12

Table S7 Sensing sequences information

Plasmids	Target gene	Sensing position	Length	Sensing sequence (5' to 3')
pRE001	HumanEEF1A	Exon 3	249	gttagcacttggctccagcatgttgtcaccattccaaccagaaattggcacaa atgctactgtgtcggggttgtagccaattttcttaatgtaagtgctgacttcctta acaatttcctcatatctcttctggctgtagggtagctcagtggaatccattttgtt aacaccgacaatgagttgtttcacacccagtgtgtaagccagaagggcaag ctctcgggtctgcccattcttggagataccagc
pRE001X	HumanEEF1A	Exon 3	249	gttagcacttggctccagcatgttgtcaccattccaaccagaaattggcacaa atgctactgtgtcggggttgtagccaattttcttaatgtaagtgctgacttcctta acaatttcctcatatctcttctggctgtagggtggctcagtggaatccattttgtt aacaccgacaatgagttgtttcacacccagtgtgtaagccagaagggcaag ctctcgggtctgcccattcttggagataccagc

Plasmids	Target gene	Sensing position	Length	Sensing sequence (5' to 3')
pTS002	HumanEEF1A	Exon 3	249	gttagcacttggctccagcatgttgtcaccattccaaccagaaattggcacaa atgctactgtgtcggggttgtagccaattttcttaatgtaagtgctgacttcctta acaatttcctcatatctcttctggctgtagggtagctcagtggaatccattttgtt aacaccgacaatgagttgtttcacacccagtgtgtaagccagaagggcaag ctctcgggtctgcccattcttggagataccagc
pTS002X	HumanEEF1A	Exon 3	249	gttagcacttggctccagcatgttgtcaccattccaaccagaaattggcacaa atgctactgtgtcggggttgtagccaattttcttaatgtaagtgctgacttcctta acaatttcctcatatctcttctggctgtagggtggctcagtggaatccattttgtt aacaccgacaatgagttgtttcacacccagtgtgtaagccagaagggcaag ctctcgggtctgcccattcttggagataccagc

Plasmids	Target gene	Sensing position	Length	Sensing sequence (5' to 3')
pTS002-ACTB	Human-ACTB	CDS	249	CTGGGTGCCAGGGCAGTGATCTCCTTCTGCATCCTGTCGGCAATGCCAGGGTACATGGTGGTGCCGCCAGACAGCACTGTGTTGGCGTACAGGTCTTTGCGGATGTCCACGTCACACTTCATGATGGAGTTGAAGGTAGTTTCGTAGATGCCACAGGACTCCATGCCCAGGAAGGAAGGCTGGAAGAGTGCCTCAGGGCAGCGGAACCGCTCATTGCCAATGGTGATGACCTGGCCGTCAGGCAGCTCG
pTS002X-ACTB	Human-ACTB	CDS	249	CTGGGTGCCAGGGCAGTGATCTCCTTCTGCATCCTGTCGGCAATGCCAGGGTACATGGTGGTGCCGCCAGACAGCACTGTGTTGGCGTACAGGTCTTTGCGGATGTCCACGTCACACTTCATGATGGAGTTGAAGGTAGTTTCGTGGATGCCACAGGACTCCATGCCCAGGAAGGAAGGCTGGAAGAGTGCCTCAGGGCAGCGGAACCGCTCATTGCCAATGGTGATGACCTGGCCGTCAGGCAGCTCG
pTS002-ARC	Human-ARC	CDS	265	cgcaggaaacgcttgagcttgggctgcagggtgcccaccacgtactggatgatctcctcctcgtccgcgtccacgtggagcgtctggtacaggtcccgcttgcgccacaggaactAgtccagcggctcgccctgcttctgcggcaggtccagctcgcgctgggtggcctctcgggacagcgtgccctcgctgtactgcaggaactccttcttgaactccacccagttcttcacggagccctgcttgaactcccaccacttcttgg

pTS002X-ARC	Human-ARC	CDS	265	cgcaggaaacgcttgagcttgggctgcagggtgcccaccacgtactgg atgatctcctcctcgtccgcgtccacgtggagcgtctggtacaggtcccg cttgcgccacaggaac**tGg**tccagcggctcgccctgcttctgcggcag gtccagctcgcgctgggtggcctctcgggacagcgtgccctcgctgtact gcaggaactccttcttgaactccacccagttcttcacggagccctgcttga actcccaccacttcttgg

Plasmids	Target gene	Sensing position	Length	Sensing sequence (5' to 3')
pTS002-PCNA	Human-PCNA	Exon 1	219	ctggtgaggttcacgcccatggccaggttgcggtcgcagcgggaggtgtc gaagccctcagaccgcagggtgagctgcaccaaagagacg**tag**gacga gtccatgctctgcaggtttacaccgctggagctaatatcccagcaggcctcg ttgatgaggtccttgagtgcctccaacaccttcttgaggatggagccctgga ccaggcgcgcctcgaac
pTS002X-PCNA	Human-PCNA	Exon 1	219	ctggtgaggttcacgcccatggccaggttgcggtcgcagcgggaggtgtc gaagccctcagaccgcagggtgagctgcaccaaagagacg**tgg**gacga gtccatgctctgcaggtttacaccgctggagctaatatcccagcaggcctcg ttgatgaggtccttgagtgcctccaacaccttcttgaggatggagccctgga ccaggcgcgcctcgaac

Plasmids	Target gene	Sensing position	Length	Sensing sequence (5' to 3')
pTS002-TP53	Human-TP53	Exon 3	279	cgtgcaagtcacagacttggctgtcccagaatgcaagaagcccagacgga aaccgtagctgccctggtaggttttctgggaagggacagaagatggcagg ggccaggaggggctggtgcaggggccgccggtgtaggagctgctAgt gcaggggccacgggggagcagcctctggcattctgggagcttcatctgg acctgggtcttcagtgaaccattgttcaatatcgtccggggacagcatcaaat catccattgcttgggacggcaaggggga
pTS002X-TP53	Human-TP53	Exon 3	279	cgtgcaagtcacagacttggctgtcccagaatgcaagaagcccagacgga aaccgtagctgccctggtaggttttctgggaagggacagaagatggcagg ggccaggaggggctggtgcaggggccgccggtgtaggagctgctggt gcaggggccacgggggagcagcctctggcattctgggagcttcatctgg acctgggtcttcagtgaaccattgttcaatatcgtccggggacagcatcaaat catccattgcttgggacggcaaggggga

Plasmids	Target gene	Sensing position	Length	Sensing sequence (5' to 3')
pTS002-XIST	Human-XIST	lncRNA	234	aaaatatggaggacgtgtcaagaagacactaggagaaagtatagaattgaa aaaaatattttatggaatttaggtgatttttttaaagaaatacgccataaagggt gttagggactagaaaatgttctagaaagaaccccaagtgcagagagatct tcagtcaggaagcttccagccccgagagagtaagaaatatggctgcagca gcgaattgcagcgctttaagaactgaa
pTS002X-XIST	Human-XIST	lncRNA	234	aaaatatggaggacgtgtcaagaagacactaggagaaagtatagaattgaa aaaaatattttatggaatttaggtgatttttttaaagaaatacgccataaagggt gttgggactagaaaatgttctagaaagaaccccaagtgcagagagatct tcagtcaggaagcttccagccccgagagagtaagaaatatggctgcagca gcgaattgcagcgctttaagaactgaa

Plasmids	Target gene	Sensing position	Length	Sensing sequence (5' to 3')
pTS003 pNeo001	MouseEef1a	Exon 3	249	gTTAGCACTTGGCTCCAGCATGTTGTCACCATT CCAACCAGAAATTGGCACAAATGCTACTGTGT CAGGGTTGTAGCCAATTTTCTTAATGTAGGTG CTGACTTCCTTAACGATTTCCTCGTATCTCTTC TGACTGTATGG**TAG**CTCGGTGGAATCCATTTT GTTGACACCAACAATCAGCTGTTTCACACCCA GGGTGTAAGCCAGAAGAGCATGCTCGCGGGT CTGCCCGTTCTTGGAGATACCAGC
pTS003X pNeo001X	MouseEef1a	Exon 3	249	gTTAGCACTTGGCTCCAGCATGTTGTCACCATT CCAACCAGAAATTGGCACAAATGCTACTGTGT CAGGGTTGTAGCCAATTTTCTTAATGTAGGTG CTGACTTCCTTAACGATTTCCTCGTATCTCTTC TGACTGTATGG**TGG**CTCGGTGGAATCCATTTT GTTGACACCAACAATCAGCTGTTTCACACCCA GGGTGTAAGCCAGAAGAGCATGCTCGCGGGT CTGCCCGTTCTTGGAGATACCAGC